

1 **Intercomparison of detection and quantification methods for methane emissions from**  
2 **the natural gas distribution network in Hamburg, Germany**

3  
4 Hossein Maazallahi<sup>1, 2</sup>, Antonio Delre<sup>3</sup>, Charlotte Scheutz<sup>3</sup>, Anders M. Fredenslund<sup>3</sup>, Stefan  
5 Schwietzke<sup>4</sup>, Hugo Denier van der Gon<sup>2</sup>, Thomas Röckmann<sup>1</sup>

6  
7 <sup>1</sup>*Institute for Marine and Atmospheric research Utrecht (IMAU), Utrecht University (UU),*  
8 *Utrecht, The Netherlands*

9 <sup>2</sup>*Netherlands Organisation for Applied Scientific Research (TNO), Utrecht, the Netherlands*

10 <sup>3</sup>*Department of Environmental Engineering, Technical University of Denmark (DTU),*  
11 *Lyngby, Denmark*

12 <sup>4</sup>*Environmental Defense Fund (EDF), Berlin, Germany*

13  
14 **Correspondence:** Hossein Maazallahi (h.maazallahi@uu.nl)

15  
16 **Abstract:**

17 In August and September 2020, three different measurement methods for quantifying methane  
18 (CH<sub>4</sub>) emission from leaks in urban gas distribution networks were applied and compared in  
19 Hamburg, Germany: the “mobile”, “tracer release” and “suction” methods.  
20 The mobile and tracer release methods determine emission rates to the atmosphere from  
21 measurements of CH<sub>4</sub> mole fractions in the ambient air, and the tracer release method also  
22 includes measurement of a gaseous tracer. The suction method determines emission rates by  
23 pumping air out of the ground using soil probes that are placed above the suspected leak  
24 location. The quantitative intercomparison of the emission rates from the three methods at a  
25 small number of locations is challenging because of limitations of the different methods at  
26 different types of leak locations.

27 The mobile method was designed to rapidly quantify the average or total emission rate of many  
28 gas leaks in a city, but it yields a large emission rate uncertainty for individual leak locations.  
29 Emission rates determined for individual leak locations with the tracer release technique are  
30 more precise because the simultaneous measurement of the tracer released at a known rate at  
31 the emission source eliminates many of the uncertainties encountered with the mobile method.  
32 Nevertheless, care must be taken to properly collocate the tracer release and the leak emission  
33 points to avoid biases in emission rate estimates. The suction method could not be completed  
34 or applied at locations with widespread subsurface CH<sub>4</sub> accumulation, or due to safety  
35 measures, and this sampling bias may be associated with a bias towards leak locations with low  
36 emission rates. The leak locations where the suction method could not be applied were the  
37 biggest emitters as confirmed by the emission rate quantifications using mobile and tracer  
38 methods and an engineering method based on leak’s diameter, pipeline overpressure and depth  
39 at which the pipeline is buried. The corresponding sampling bias for the suction technique led  
40 to a low bias in derived emission rates in this study. It is important that future studies using the  
41 suction method account for any leaks not quantifiable with this method in order to avoid biases,  
42 especially when used to inform emission inventories.

# 1 Introduction

Natural gas combustion has a lower carbon footprint than combustion of other fossil fuel sources for the same thermal output (EIA, 2021). However, fugitive methane (CH<sub>4</sub>) emissions can significantly turn the balance in terms of climate impact (Alvarez et al., 2012) because the global warming potential of CH<sub>4</sub> over a 20-year time scale is 84 times higher than that of carbon dioxide (CO<sub>2</sub>) (Myhre et al., 2013). The atmospheric abundance of CH<sub>4</sub> has increased about 2.5-fold since the pre-industrial era (Bousquet et al., 2006). Following a short period of stable levels after the year 2000, atmospheric CH<sub>4</sub> has continued to increase since 2006. Worden et al (2017) concluded that about 50 to 80% of the post-2006 increase originated from fossil sources and Jackson et al. (2020) attributed the accelerated increase of 6 – 13 ppb yr<sup>-1</sup> from 2014 to 2017 (Nisbet et al., 2019), equally to the emission increase from fossil and agriculture sectors.

Gas distribution networks in cities are subject to maintenance programs by the operators to detect and fix leakages that occur, as CH<sub>4</sub> is an incendiary gas and can be explosive at concentrations between 4 and 16% in ambient air (DVGW, 2022). Since the safe operation of the distribution network and leak repair is the primary objective of this maintenance, quantification of emissions from leakages is rarely performed. The absence of regulations on CH<sub>4</sub> emissions is another reason why leak rates are not routinely quantified, however CH<sub>4</sub> emissions from the energy sector needs to be addressed properly within the EU CH<sub>4</sub> strategy by 2050 (EC, 2020). Nevertheless, from the perspective of climate change and possible mitigation options, it is important that emissions from gas leakages are (i) quickly detected and fixed and (ii) well quantified. Weller et al. (2020) and Alvarez et al. (2018) respectively reported 5 and 1.6 times higher CH<sub>4</sub> emissions from leaks in the US gas distribution network based on such observations compared to the national inventory reports.

Leaks from buried pipelines can be due to corrosion or failure/defects in joints or materials (EPA, 1996). When a leak occurs on a buried urban gas pipeline, the gas will generally accumulate in the air space below the surface and then find its path to the atmosphere through a single or several surface outlets. The outlets can be either unpaved soil surfaces, cracks in the road or pavements, or associated with different types of cavities (manholes, communication covers, rain drains, etc.). The major outlet is generally the one with the highest overall permeability for gas released from the buried natural gas pipeline. On the way from the leak location on a buried pipeline to the atmosphere through outlets, CH<sub>4</sub> may be oxidized by methanotrophs in the soil and/or merge with CH<sub>4</sub> from other sources, e.g. biogenic CH<sub>4</sub> emissions from sewage system.

Routine leak surveys in Germany are conducted by walking with handheld CH<sub>4</sub> sensors above buried pipelines, referred to as the carpet method (DVGW, 2019). The success of leak detection with the carpet method depends primarily on soil permeability (Ulrich et al., 2019), which is influenced by soil moisture, texture, soil organic content and the location of the groundwater table (Wiesner et al., 2016). Based on risk of explosion, gas leaks are classified into four types: A1, A2, B and C (DVGW, 2019). This classification is based on the accumulation of CH<sub>4</sub> in cavities (e.g. manholes, rain drains, etc.) or buildings and the distance of gas leaks to buildings and cavities. If natural gas leaks into buildings or cavities, the leak classifies as A1, and it must be repaired immediately to minimize explosion risk. If the gas leak has a distance up to 1 m to buildings and does not fill cavities, it is classified as A2, and it must be fixed within a week. If the distance is between 1 to 4 m to buildings, the leak is classified as B and the repair time

97 window is three months, and if the distance is more than 4 m then, the leak is considered as C  
98 category and can be fixed according to the scheduled repair plan. There are 6,500 km of low  
99 pressure and 250 km of medium pressure gas pipelines in Hamburg which are monitored every  
100 4 years with the carpet method based on the national regulations in Germany. Gas leaks in  
101 cities are not quantified and thus also not a parameter affecting the course of action. Moreover,  
102 high pressure pipelines are monitored on annual basis with additional helicopter-based  
103 measurement platform.

104  
105 In recent years, mobile measurement methods using vehicles with fast and high-precision laser  
106 instrumentation have been established for leak detection and emission quantification in  
107 numerous cities (Fernandez et al., 2022; Defratyka et al., 2021; Luetschwager et al., 2021;  
108 Keyes et al., 2020; Maazallahi et al., 2020; Ars et al., 2020; Weller et al., 2018; von Fischer et  
109 al., 2017; Jackson et al., 2014). In-situ measurements of atmospheric CH<sub>4</sub> from mobile vehicles  
110 are used to pinpoint and quantify CH<sub>4</sub> emission sources at street level in urban areas. The  
111 mobile method was calibrated using above-ground controlled release experiments, in which  
112 known amounts of CH<sub>4</sub> were released from gas cylinders (Weller et al., 2019). Simultaneous  
113 measurements of carbon dioxide (CO<sub>2</sub>) and ethane (C<sub>2</sub>H<sub>6</sub>) can provide valuable additional  
114 information for attributing CH<sub>4</sub> sources (Maazallahi et al., 2020). A characteristic of the  
115 resulting emissions distribution from gas distribution grids in cities is the existence of a few  
116 leak locations with very high leak rates, up to 100 L min<sup>-1</sup>, resulting in a right-skewed leak  
117 emission rate distribution (Weller et al., 2020). Usually about 10% of the leaks are responsible  
118 for between 30% to 70% of the emissions (Weller et al., 2019; Maazallahi et al., 2020).  
119 Therefore, the CH<sub>4</sub> emission from the gas distribution system can be reduced very effectively  
120 if the largest leaks can be found and fixed quickly, thus augmenting the routine leak detection  
121 (carpet method) and repair programs with the mobile method.

122  
123 The tracer dispersion method is another method to quantify CH<sub>4</sub> emissions from point and area  
124 sources. In this method, a tracer gas is released at a known rate close to the outlet of the gas  
125 leak, and both tracer and target gas concentrations are measured downwind. From these  
126 measurements and the known tracer gas release rate, the target gas emission rate can be  
127 determined with an uncertainty of ± 15% (Lamb et al., 1995) or less than 20% (Fredenslund et  
128 al., 2019). Lamb et al. (2015) applied the tracer method to quantify leaks from urban  
129 underground pipelines where they reported moderate agreement (± 50%) to excellent  
130 agreement (± 5%) between the tracer and high-flow sampler method.

131  
132 Another approach to quantify underground leak rates from buried gas pipelines is the so-called  
133 suction method. In this method air is pumped out of the ground at a known rate via probes  
134 surrounding the underground leaks until an equilibrium CH<sub>4</sub> mixing ratio is reached in air out-  
135 flow, from which the CH<sub>4</sub> leak rate can be calculated. In Germany, this approach is applied to  
136 a limited number of leak locations, which do not have to be repaired immediately or within 1  
137 week. Suction measurements normally find leak rates that are < 2 L min<sup>-1</sup> (E.ON, personal  
138 communication, 2020). The reported uncertainty range of this method is ± 10% based on 23  
139 measurements in the 1990s (E.ON, personal communication, 2020). The discrepancy between  
140 these rather low leak rates compared to leak rates inferred with the mobile method calls for  
141 further investigation, since the suction method is also employed to derive network-wide  
142 emission factors for the German country-wide gas distribution network (Federal Environment  
143 Agency, 2020).

144  
145 Hendrick et al. (2016) used surface flux chamber measurements carried out between 2012 and  
146 2014 to estimate gas leak rates from 100 leak locations in the Boston area that were detected

147 using mobile measurements ( $n = 45$ ) in 2011 from Phillips et al. (2013) and additional locations  
148 from later mobile surveys ( $n = 55$ ). They reported  $\text{CH}_4$  emission rates from gas leaks ranging  
149 from  $0.003 \text{ g min}^{-1}$  to  $16 \text{ g min}^{-1}$ , corresponding to roughly  $0.0 - 24.4 \text{ L min}^{-1}$ . They also  
150 reported that their estimate using chamber measurements underestimated total  $\text{CH}_4$  emissions,  
151 likely because the chambers didn't capture the total  $\text{CH}_4$  emitted from the leak. This is similar  
152 to the enclosure measurements results from Weller et al. (2018).

153

154 The flow through a hole in a pipeline can also be calculated theoretically and empirically from  
155 the physical properties of the hole, mainly the ratio of hole to pipeline diameter and the  
156 overpressure in the pipeline. There are three different engineering model types to estimate  
157 emissions from gas leaks: the hole model, the rupture model and modified models to bridge the  
158 gap between hole and rupture models (Hu et al., 2020; Moloudi and Esfahani, 2014; Yuhua et  
159 al., 2002; Arnaldos et al., 1998). These types of models are either to estimate leak strength from  
160 a pipeline in open space or a buried pipeline. A leak on a buried pipeline has higher surrounding  
161 resistance depending on soil conditions compared to a situation where the pipeline is in open  
162 space. Such models have been used to quantify emissions from holes in pipelines in open space  
163 (Hou et al., 2020; Manda and Morshed, 2017; Moloudi and Esfahani, 2014; Mahgerefteh, Oke  
164 and Atti, 2005; Yuhua et al., 2003; Kayser and Shambaugh, 1991) but also from buried  
165 pipelines (Liu et al., 2021; Ebrahimi-Moghadam et al., 2018; Okamoto and Gomi, 2011; Yan,  
166 Dong and Li, 2015). Cho et al. (2021) introduced a model, which takes into account soil  
167 properties including absolute and relative permeability and porosity, the underground spread  
168 of the leak, surface  $\text{CH}_4$  mole fractions and depth of the buried pipeline based on experiments  
169 with a controlled release rate. This model was calibrated based on release rates ranging from  
170  $1.3 \text{ g min}^{-1}$  to  $5.7 \text{ g min}^{-1}$ , corresponding to roughly  $2.0 - 8.7 \text{ L min}^{-1}$ .

171

172 In this study, we present results from measurements with the mobile, the tracer release and the  
173 suction methods in Hamburg, Germany, in August and September 2020. We present the  
174 quantitative emission estimates as well as a qualitative intercomparison of the three methods,  
175 in particular related to the applicability and the strengths and weaknesses of the different  
176 methods at different leak locations. We investigate differences between the leaks detected from  
177 mobile measurements and leak locations reported from the routine leak detection surveys  
178 performed by the local gas utility (hereinafter LDC (Local Distribution Company)). Finally,  
179 we discuss implications of our study for national emission inventories.

180

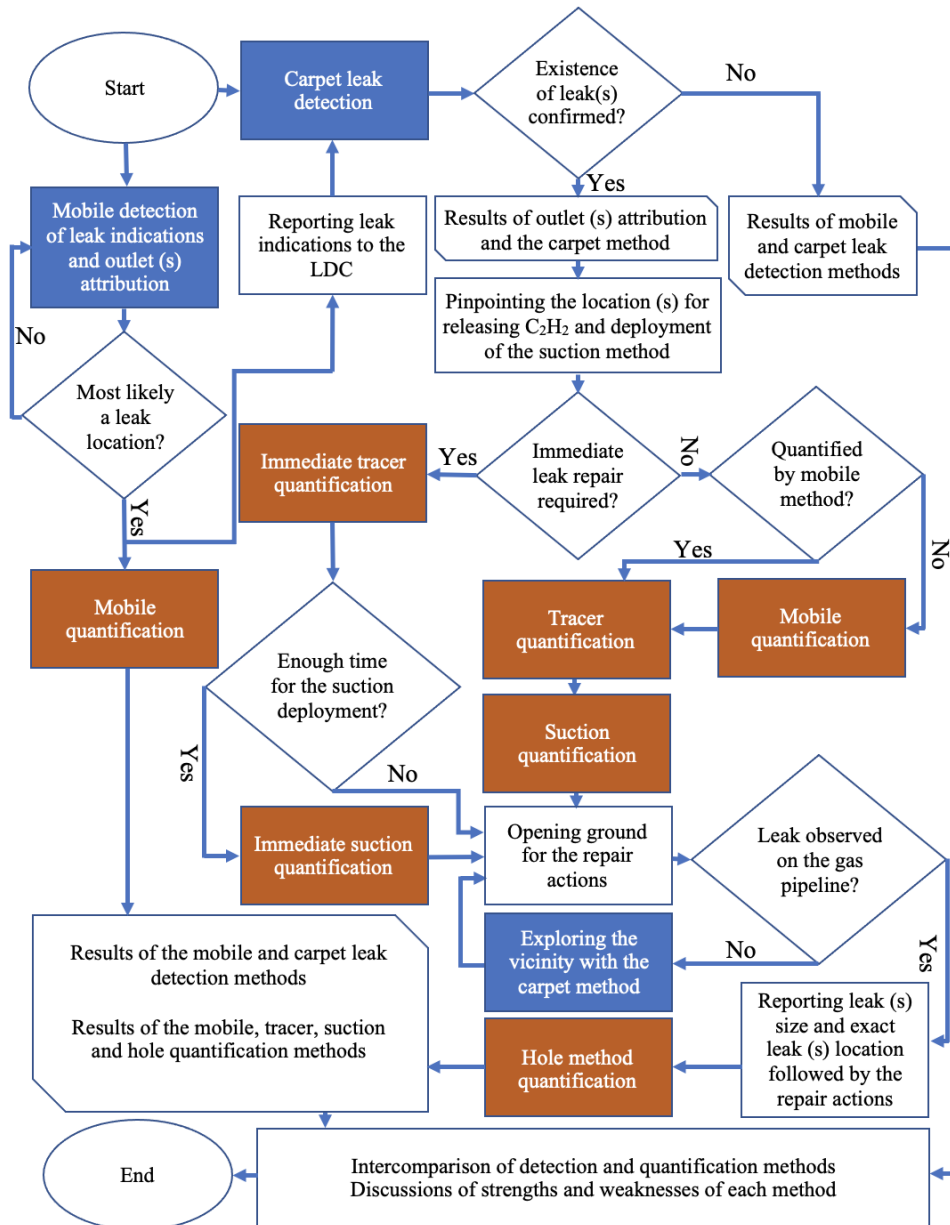
## 181 **2 Materials and Methods**

### 182 **2.1 Campaign preparation and general overview**

183 As a preparation for the intercomparison campaign, all partners contributed to the preparation  
184 of an "intercomparison matrix" where the characteristics and deployment details of the  
185 different methods were specified. This matrix is provided in section S.1 of the Supplemental  
186 Information (SI). The matrix includes descriptions related to the identification of gas leaks, the  
187 quantification of gas leaks, adjustments of the method to the intercomparison exercise and  
188 upscaling. It also laid out an initial plan for the intercomparison in terms of identification of  
189 suitable locations and deployment of the different methods.

190 According to this plan (Fig. 1), we first applied the mobile method to identify potential gas leak  
191 locations, namely leak indications (LIs). When the mobile method had detected one or more  
192 emission outlets (See Sect. S.2 in SI) and classified them as a potential gas leak location, the  
193 carpet method was applied to confirm the leak and determine the confine leak location. Some  
194 additional locations that had previously been identified by the carpet method (leak categories  
195 B and C) were added to the list of target locations.

196 Following leak detection, the mobile quantification method (multiple transects) was applied on  
 197 all the locations and the tracer and suction methods were applied at the confirmed leak  
 198 locations, and with some restrictions regarding safety and method capacities. The release  
 199 location for the tracer quantification method was confirmed based on surface screening using  
 200 a handled methane analyzer. For comparison of the mobile and tracer release methods with the  
 201 suction and hole methods we assumed that (i) a steady state between pipeline leakage under-  
 202 ground CH<sub>4</sub> accumulation and emission to the atmosphere had been reached (Kirchgessner et  
 203 al., 1997) and (ii) methanotrophs and methanogens have negligible impact on quantification of  
 204 gas leak emissions. Thus, the total emission rate of all outlets in the vicinity of a leak location  
 205 is equal to the natural gas emission rate from the pipeline leak. We will discuss implications of  
 206 the above assumptions for selected cases. After leak repair, the LDC reported leak hole sizes,  
 207 pipeline diameters and pipeline operational pressures, allowing leak rate estimation with the  
 208 hole method.



209  
 210 **Figure 1 – Flowchart of application of leak detection methods (blue colors) and**  
 211 **quantification methods (red colors) followed by repair actions and intercomparison of**  
 212 **the detection and quantification methods**

## 213 **2.2 Measurements setups**

### 214 **2.2.1 Mobile measurement setup**

215 Onboard the measurement vehicle (VW Transporter) we operated two cavity ring-down  
216 spectrometers (CRDS), model G2301 and model G4302 (Picarro, Santa Clara, California,  
217 USA). The G2301 measures CH<sub>4</sub>, CO<sub>2</sub> and water vapor (H<sub>2</sub>O) at a flow rate of  $\approx 0.2 \text{ L min}^{-1}$   
218 and 0.3 Hz frequency. The G4302 has a flow rate of  $\approx 2.2 \text{ L min}^{-1}$  and sampling frequency of  
219 about 1 Hz for CH<sub>4</sub>, C<sub>2</sub>H<sub>6</sub> and H<sub>2</sub>O. The air intake for both instruments was from the same  
220 tubing attached to the front bumper. This setup allowed us to directly compare the  
221 enhancements observed from the two instruments during surveys. The G4302, which is in a  
222 shape of a backpack, was also used in attribution of outlets emissions in walking surveys to  
223 check presence of C<sub>2</sub>H<sub>6</sub> in emission outlets.

224

### 225 **2.2.2 Tracer release measurement setup**

226 The tracer release method was applied by releasing acetylene (C<sub>2</sub>H<sub>2</sub>) at the emission outlet  
227 identified by the mobile leak detection and confirmed by the carpet method. The tracer gas  
228 was released at the main emission outlet, which was confirmed by surface screening using a  
229 handheld CH<sub>4</sub> analyzer. Tracer release rates between 1.3 and 2.6 L min<sup>-1</sup> from a gas cylinder.  
230 A Picarro CRDS, G2203 instrument was used to measure CH<sub>4</sub> and C<sub>2</sub>H<sub>2</sub> mole fractions  
231 continuously with  $\approx 0.3 \text{ Hz}$  frequency. The instrument was installed in a measurement vehicle  
232 (VW Caddy), and air was sampled from the atmosphere through an inlet on the roof about 2m  
233 above ground. The tracer method was applied either in static mode, where air was sampled in  
234 one or a few locations downwind from the outlets and tracer release locations (n = 11) or mobile  
235 mode (n = 5), where the plumes were transected while measuring concentrations of CH<sub>4</sub> and  
236 C<sub>2</sub>H<sub>2</sub>. The choice of mode depended on the site conditions including road accessibility and  
237 wind direction. The tracer release setup including instrumentation used as well as mobile mode  
238 is described in detail in Mønster et al (2014), and the principle of the static mode is described  
239 in Fredenslund et al (2010).

240

### 241 **2.2.3 Suction measurement setup**

242 In the suction method, 12 probes were used to insert in the soil around the confirmed gas leak  
243 location by the LDC. The probes are connected to a pump to extract accumulated subsurface  
244 CH<sub>4</sub> from the leak. CH<sub>4</sub> mole fraction at the outflow is measured with a Flame Ionization  
245 Detector (MEEM, 2018).

246

### 247 **2.2.4 Carpet method setup**

248 Leak detection experts from the LDC operate a methane detector (Sewerin instruments,  
249 Gütersloh, Germany) on a rolling device, where a plastic cover (the carpet) moves over the  
250 ground and provides a loose seal to the surrounding atmosphere, facilitating preferential  
251 analysis of air emanating from the surface right below the carpet. The instrument gives an  
252 acoustic signal when a high CH<sub>4</sub> from a potential leak has been detected. The instrument can  
253 detect C<sub>2</sub>H<sub>6</sub> with a gas chromatograph, which take about couple of minutes per outlet location.

254

## 255 **2.3 Detection, confirmation and attribution of emissions at gas leak locations**

### 256 **2.3.1 Mobile detection of possible leak location**

257 For leak detection with the mobile method, we first evaluated CH<sub>4</sub>, C<sub>2</sub>H<sub>6</sub> and CO<sub>2</sub> signals  
258 during mobile surveys. If (i) CH<sub>4</sub> and C<sub>2</sub>H<sub>6</sub> signals were observed with a ratio of less than 10%  
259 with no CO<sub>2</sub> signal or (ii) CH<sub>4</sub> was observed (< 500 ppb enhancement on G4302) with no C<sub>2</sub>H<sub>6</sub>  
260 and CO<sub>2</sub> signals, then we parked the mobile measurement car, detached the G4302 analyzer  
261 from the system and searched for gas outlets on foot with the G4302. This detailed search for  
262 outlets was performed to (i) confirm the presence of both CH<sub>4</sub> and C<sub>2</sub>H<sub>6</sub> signals (ii) map the

263 spatial spread of outlets and (iii) spatially constrain the possible gas leak location. The reported  
264 possible gas leak locations from the mobile method were then reported to the LDC for  
265 confirmation and localization of the leak with the carpet method and subsequent underground  
266 measurements.

267

### 268 **2.3.2 Attribution of leak indication signals from mobile measurements**

269 To attribute an observed leak indication (LI) from mobile measurements to a source category,  
270 namely fossil, microbial and combustion, we used CO<sub>2</sub> and C<sub>2</sub>H<sub>6</sub> signals, which were  
271 continuously measured along with CH<sub>4</sub>. We quantitatively evaluated C<sub>2</sub>:C<sub>1</sub> ratios (%) when (i)  
272 the CH<sub>4</sub> enhancements were larger than 0.5 ppm (ii) C<sub>2</sub>H<sub>6</sub> enhancements were also larger than  
273 15 ppb and (iii) the determination coefficient (R<sup>2</sup>) of the linear regression between CH<sub>4</sub> and  
274 C<sub>2</sub>H<sub>6</sub> was larger than 0.7. If CH<sub>4</sub> signals in mobile measurements were associated with CO<sub>2</sub>  
275 and high C<sub>2</sub>H<sub>6</sub> mole fractions (C<sub>2</sub>:C<sub>1</sub> > 10%), we attributed those emissions to combustion  
276 (Maazallahi et al., 2020). When we repeatedly observed CH<sub>4</sub> enhancements, no CO<sub>2</sub>  
277 enhancements and C<sub>2</sub>:C<sub>1</sub> ratios between 1 and 10%, or we observed persistent CH<sub>4</sub> signals in  
278 several passes we did further on-foot inspection of the outlets. If the emissions from the outlets  
279 clearly pointed to a fossil origin based on the CH<sub>4</sub> and C<sub>2</sub>H<sub>6</sub> signals, we labeled the locations  
280 as potential gas leak locations and reported them to the LDC for confirmation. We only  
281 considered a location as a gas leak for further investigation if the LDC confirmed the existence  
282 of a gas leak.

283 If at a particular location, we observed several CH<sub>4</sub> maxima, for example from different outlets,  
284 we considered the “strongest” outlet as the main emission point. The “strongest” emission point  
285 refers to a point where we observed the highest CH<sub>4</sub> mole fraction when the G4302 intake inlet  
286 was put at a distance of ≈ 2 - 5 cm above the surface or outlet. When several emission outlets  
287 with similar mole fractions were found, we considered the spatial average of the coordinates  
288 as the main emission point. The tracer method then released C<sub>2</sub>H<sub>2</sub> at the main outlet emission  
289 point.

290 The LDC reported a C<sub>2</sub>:C<sub>1</sub> ratio of 3.0% (96.20 ± 0.02 mol % CH<sub>4</sub> and 2.88 ± 0.00 mol %  
291 C<sub>2</sub>H<sub>6</sub>, GNH personal communication) for the gas composition in the grid for the period of  
292 August and September 2020 in Hamburg. This ratio was reported 3.5% (95.09 mol % CH<sub>4</sub> and  
293 3.37 mol %, GNH personal communication) in April 2020.

294

### 295 **2.3.3 LDC leak detection and confirmation**

296 Since the pipeline locations are known to the LDC, the method can be applied precisely above  
297 the pipelines, including visible cracks and cavity outlets in the close vicinity, increasing the  
298 possibility of leak detection. Once the carpet method detects a CH<sub>4</sub> source, a second  
299 measurement is performed above the location with the highest signal, where air is accumulated  
300 and analyzed for the presence of C<sub>2</sub>H<sub>6</sub>. The C<sub>2</sub>H<sub>6</sub> detection in the carpet method is not online  
301 with higher detection threshold and in batch mode (gas chromatography), which takes time, 5  
302 – 10 minutes per location. If sufficiently high CH<sub>4</sub> and C<sub>2</sub>H<sub>6</sub> levels are found, the leak is  
303 categorized in one of safety categories of A1, A2, B or C.

304

### 305 **2.3.4 Precise underground leak localization**

306 When a leak has been confirmed with the carpet method, a precise localization of the leak is  
307 performed by drilling holes about 20-40 cm into the ground along the pipeline track and  
308 measuring the sub-surface CH<sub>4</sub> concentration. The location with the maximum sub-surface  
309 reading is assigned the most likely leak location where the repair teams open the road and  
310 attempt repair of the leak. The final exact leak location is reported after opening ground for the  
311 repair reactions. Mostly the locations reported from the carpet method matches the locations

312 reported from the leak repair team, which depends on the transport pathways of emission  
313 undersurface and surface coverage.

314

## 315 **2.4 Emission quantification**

### 316 **2.4.1 Mobile measurements quantifications**

317 After the detection of the target locations, we performed additional transects at these locations  
318 on different days. We accepted a mobile measurement transect of a leak location for further  
319 analysis if (i) the GPS signals of transects were logged correctly along the street track and (ii)  
320 at least one of the two instruments, G2301 (for quantification and attribution) and / or G4302  
321 (for attribution), were running during the transect and (iii) the transect track included at least  
322 one GPS coordinate less than 50 m from the leak location. The start and end point of the  
323 accepted transects were determined as the locations where the driving tracks intersected with a  
324 circle with radius of 100 m centered at the gas leak location reported by the LDC, or a reported  
325 outlet location from the mobile method, for the locations where the LDC did not confirm a  
326 leak. The segments between the start and end points were evaluated one by one (See an example  
327 in Sect. S.4.1 in SI) to determine various parameters, e.g., the maximum CH<sub>4</sub> enhancements,  
328 plume area, driving speed, distance to the actual leak locations, etc. The plume area is the  
329 integral of the CH<sub>4</sub> enhancements above background along the driving track from the location  
330 where the CH<sub>4</sub> enhancement exceeds > 10 ppb until the location where it falls again below the  
331 10 ppb threshold.

332 Gas leak quantification from mobile measurements is based on an empirical equation derived  
333 from controlled release experiments reported by von Fischer et al., (2017) and reevaluated in  
334 Weller et al., (2019) (Eq. 1).

335

$$336 \quad Q = \exp (\overline{\ln (C_{max})} + 0.988) / 0.817 \quad \text{Eq. 1}$$

337

338 In Eq. 1,  $C_{max}$  is the maximum CH<sub>4</sub> enhancement (ppm) observed during each transect next to  
339 the leak location. The maximum CH<sub>4</sub> enhancement should be more than 10% above CH<sub>4</sub>  
340 background level to be considered for the quantification algorithm. The emission rate is  
341 denoted by Q and it is in L min<sup>-1</sup>.  $\overline{\ln (C_{max})}$  is the mean of the logarithm of the maximum  
342 mole fraction enhancements for all accepted transects.

343 The standard quantification method only uses transects where CH<sub>4</sub> enhancements are more  
344 than 10% or  $\approx 200$  ppb above background level. This 10% enhancement threshold corresponds  
345 to about 0.5 L min<sup>-1</sup> emission rate in Eq. 1. Thus,  $\approx 0.5$  L min<sup>-1</sup> is the minimum emission rate  
346 that can be quantified with Eq. 1 and leaks with smaller emission rates are ignored by design  
347 of the method. Below we investigate the effect of relaxing the enhancement threshold. The  
348 application of the tracer release technique in mobile mode allowed us to use the known C<sub>2</sub>H<sub>2</sub>  
349 release rate and the measured C<sub>2</sub>H<sub>2</sub> plumes to independently validate the mobile approach,  
350 including the effect of the enhancement threshold. We also investigated the effect of distance  
351 between CH<sub>4</sub> maxima to gas leak locations, which is not a parameter in Eq. 1.

352 The uncertainty of the emission rate for each location in the mobile method was calculated  
353 using standard error and t-factor (95% confidence) for the locations with at least three CH<sub>4</sub>  
354 enhancements greater than the 10% threshold.

355 In addition to evaluating the maximum CH<sub>4</sub> enhancement from each transect we also derived  
356 the plume area (mixing ratio times distance and in unit of ppm m) for comparison between the  
357 instruments. In principle, the plume area should provide a more robust quantification of an  
358 ambient CH<sub>4</sub> plume than the maximum enhancement: When a plume spreads out, individual  
359 realizations of the plume can be sharper and higher, or wider and lower, depending on  
360 meteorological conditions, but the plume area should be less affected. In addition, when an  
361 instantaneous plume is sampled with two instruments with different gas flow rates, instruments



362 with a lower flow rate will be affected by mixing of air in the measurement cell. This will lead  
 363 to a lower maximum enhancement but a wider peak, and thus the peak area should lead to a  
 364 better comparison between the instruments.

365

#### 366 **2.4.2 Tracer measurements quantifications**

367 The tracer method uses Eq. 2a to quantify CH<sub>4</sub> emissions in mobile mode (integral over space  
 368 dimension) and Eq. 2b in the static mode (integral over time dimension). Parameters relevant  
 369 for the evaluation with the tracer method are provided in Sect. S.4.2.

$$370 \quad Q_{CH_4} = Q_{C_2H_2} \cdot \frac{\int_{start}^{end} C_{CH_4} dx}{\int_{start}^{end} C_{C_2H_2} dx} \cdot \frac{MW_{CH_4}}{MW_{C_2H_2}} \quad \text{Eq. 2a}$$

$$371 \quad Q_{CH_4} = Q_{C_2H_2} \cdot \frac{\int_{start}^{end} C_{CH_4} dt}{\int_{start}^{end} C_{C_2H_2} dt} \cdot \frac{MW_{CH_4}}{MW_{C_2H_2}} \quad \text{Eq. 2b}$$

372

373 Here C is the mole fraction (ppm) and MW is the molecular weight of the species, 16 g mol<sup>-1</sup>  
 374 for CH<sub>4</sub> and 26 g mol<sup>-1</sup> for C<sub>2</sub>H<sub>2</sub>.  $Q_{CH_4}$  is the CH<sub>4</sub> emission rate estimate for CH<sub>4</sub> (g s<sup>-1</sup>) and  
 375  $Q_{C_2H_2}$  is the controlled release rate of C<sub>2</sub>H<sub>2</sub> (g s<sup>-1</sup>). The C<sub>2</sub>H<sub>2</sub> flow rate was controlled and  
 376 measured with a flow controller (Brooks Sho-Rate). In addition, the mass of C<sub>2</sub>H<sub>2</sub> released at  
 377 each location was measured by weighing the release cylinder before and after the tracer release  
 378 with a precise scale (KERN DE60K5A). The change in mass was then converted to a mass  
 379 flow rate using the release time. To convert the emission rate from mass (g s<sup>-1</sup>) to volume (L  
 380 min<sup>-1</sup>) we used normal temperature and pressure (NTP) conditions, T = 293.15 K, p = 1.01325  
 381 bar. The locations of tracer release (C<sub>2</sub>H<sub>2</sub>) at the confirmed gas locations were determined with  
 382 the combined information from the mobile and the carpet methods.

383 The tracer gas can also be used to pinpoint and confirm the emission source location. Prior to  
 384 quantification, it is important that the emission outlet is located for proper tracer release (see  
 385 Fig. 1) and source simulation and that other potential interfering emission sources can be ruled  
 386 out. This is secured by performance of upwind and downwind CH<sub>4</sub> mole fraction screening.  
 387 During transecting of the CH<sub>4</sub> and tracer plumes, the two plumes should match, if this is not  
 388 the case, the tracer release should be relocated until a proper plume match is obtained. If an  
 389 emission source consists of multiple outlets, the combined emission from all outlets can be  
 390 measured by releasing the tracer at the main outlet and increasing the measuring distance until  
 391 one confined overlapping plume of CH<sub>4</sub> and tracer gas is obtained. If the distance cannot be  
 392 increased to access limitations, tracer should be released at each single emission outlet.

393

#### 394 **2.4.3 Suction measurements quantifications**

395 The quantification of a leak with suction method is possible after pumping accumulated air out  
 396 of soil and reaching CH<sub>4</sub> mole fraction equilibrium in the outflow. With the equilibrium CH<sub>4</sub>  
 397 reached and the known pumping rate through the probes, it is then possible to calculate  
 398 emission rate (See Sect. S.4.3 in SI).

399

#### 400 **2.4.4 Hole method, based on leak and pipeline properties**

401 The LDC reported the physical properties of gas leaks and pipeline conditions. These include  
 402 leak area, pipeline diameter and pipeline operational pressure. In order to get an estimate of the  
 403 upper physical limits of gas leakage through a hole with the given properties, we used the  
 404 empirical model by Liu et al., (2021), which was designed to quantify emissions from buried  
 405 natural gas pipelines to estimate emission rates from the leaks (Eq. 3), hereinafter “hole”  
 406 method.

407

408  $Q = 0.567 \cdot [(h + 139.592)^{-0.1} - 0.542] \cdot d^{1.5} \cdot p^{0.7}$  Eq. 3

409

410 Here, Q is the gas leak rate in  $\text{m}^3 \text{h}^{-1}$  (at standard atmospheric conditions and converted to  
 411 NTP), h is the depth of the buried pipeline in cm, d is the gas leak hole diameter in mm and p  
 412 is the pipeline overpressure in kPa. We used 150 cm as pipeline depth for all the locations in  
 413 Hamburg to estimate emission rate. We note that the model that we employed is for buried  
 414 pipelines not pipelines in open space, and emission estimates for the gas leak emission rate in  
 415 open space would be even higher (See Sect. 4.4 in SI). Ebrahimi-Moghadam et al. (2018)  
 416 showed that  $\text{CH}_4$  emission from a pipeline hole area can be between 7 to 10 times higher in  
 417 open space relative to the subsurface conditions.

418

### 3 Results

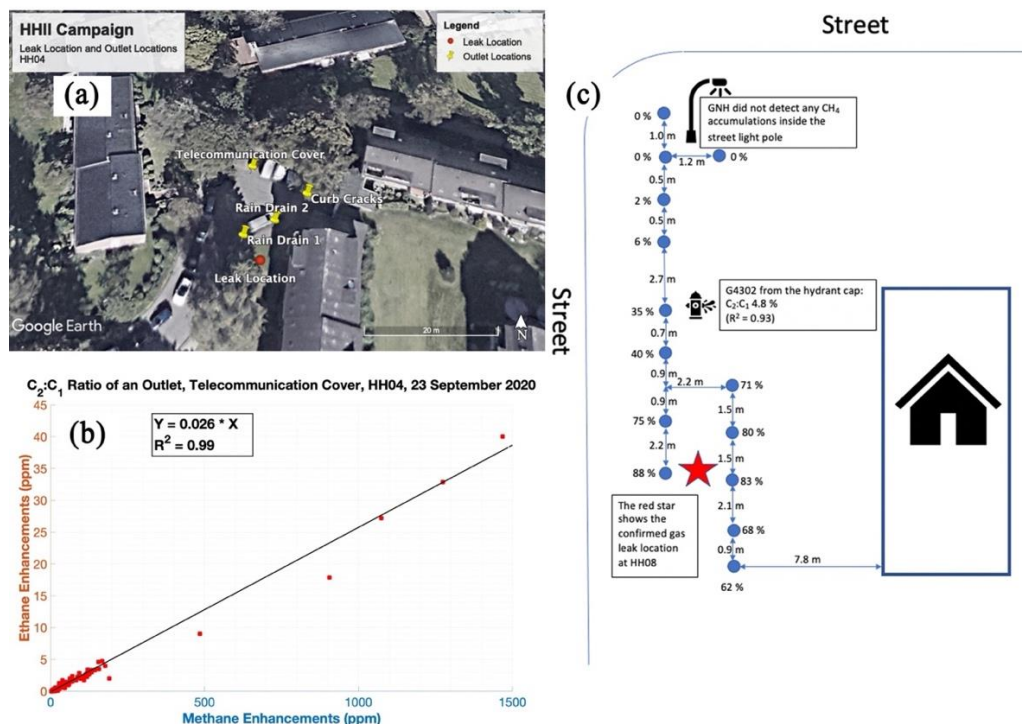
419

420

#### 3.1 Leak Detection

421

422 15 possible leak locations were detected by the mobile method in the initial surveys, (labeled  
 423 as HH001 – HH015). At 13 out of these 15 locations, leaks were confirmed by the LDC, HH007  
 424 and HH012 locations were not confirmed as gas leak locations. In addition, the LDC identified  
 425 5 other leak locations (labeled as HH100 – HH104) that had not yet been fixed (category B and  
 426 C). The overview of the measurements (detection and quantification) is provided in the SI (See  
 427 Sect. S.5 in SI). At some locations we also observed that vegetation was impacted negatively  
 428 by the presence of leaks in their vicinities, a known phenomenon as high levels of methane  
 429 cause harmful anoxic conditions for the plant roots (See Sect. S.6 in SI). At several locations  
 430 the outlet identification was straightforward, because we only observed one outlet, but at 5  
 431 locations we observed numerous outlets spread over a large area. Figure 2 shows the spread of  
 432 emission outlets at one of the locations (Fig. 2a), with correlations of  $\text{CH}_4$  and  $\text{C}_2\text{H}_6$  at the  
 433 “strongest” outlet (Fig 2b). Fig. 2c shows precise gas leak location practice of the LDC at one  
 434 of the other locations.



435

436 **Figure 2 – (a) aerial image of location HH004 (© Google Maps). Yellow pins show surface**  
 437 **emission outlet locations, and the red point shows the actual pipeline leak location**

438 reported by the LDC; (b) correlation between CH<sub>4</sub> and C<sub>2</sub>H<sub>6</sub> measured from a  
 439 telecommunication cover; (c) Map (not to scale) of drilled holes (blue dots) to locate the  
 440 pipeline gas leak at HH008. The red star shows the actual pipeline gas leak location as  
 441 indicated by the undersurface CH<sub>4</sub> mole fractions (See Sect. S.3, Fig. S3)  
 442

### 443 3.2 Leak Quantification

444 Table 1 shows the results of the leak emission rate quantifications from the four methods. All  
 445 these locations were quantified by the mobile method, although for 6 of them the 10%  
 446 enhancement threshold was not reached. 16 locations were quantified by the tracer release  
 447 method and 8 by the suction method. A complete overview of key parameters for all  
 448 measurements (detection and quantification) is provided in Sect. S.5.  
 449

450 Table 1 – Results of gas leak quantification with different methods in Hamburg, Germany

|                           | ID                              | Leak quantification methods (L min <sup>-1</sup> )            |                     |   |                                  |                                    |        | Info. from the LDC             |                         |                              |                                     |                                |
|---------------------------|---------------------------------|---|---------------------|---|----------------------------------|------------------------------------|--------|--------------------------------|-------------------------|------------------------------|-------------------------------------|--------------------------------|
|                           |                                 | Mobile<br>(measurements from G2301)                           |                     |   | Tracer<br>(L min <sup>-1</sup> ) | Suction                            |        | Hole<br>(L min <sup>-1</sup> ) | Pipeline buried<br>year | Leak size (cm <sup>2</sup> ) | Leak type; Safety<br>considerations | Pipeline Size and<br>Material# |
|                           |                                 | Transect (s)<br>w/ CH <sub>4</sub> Enh.<br>> 10%<br>threshold | Emission<br>average | Emission<br>range;<br>95%<br>confidence |                                  | Emission<br>(L min <sup>-1</sup> ) | Status |                                |                         |                              |                                     |                                |
| Detected by mobile method | HH001                           | n = 1 (10%)   | 0.7                 | -                                       | 0.06                             | <1.8                               | INC    | 39                             | 1935                    | 2.5                          | C                                   | DN80ST                         |
|                           | HH002                           | n = 5 (50%)   | 4.9                 | 0.7 – 36.0                              | 0.22                             | <0.7                               | INC    | 45                             | 1935                    | 3.0                          | A2                                  | DN80ST                         |
|                           | HH003                           | n = 6 (86%)   | 7.5                 | 1.1 – 53.0                              | 1.37                             | -                                  | -      | -                              | 1963                    | -                            | A1                                  | DN100ST                        |
|                           | HH004                           | n = 4 (100%)  | 7.8                 | 1.8 – 34.5                              | 5.33                             | -                                  | -      | -                              | 1959                    | -                            | A1                                  | DN80ST                         |
|                           | HH005 <sup>+</sup>              | n = 19 (51%)  | 1.8                 | 0.9 – 3.6                               | 0.21                             | -                                  | -      | -                              | 1935                    | -                            | A2                                  | DN80ST                         |
|                           | HH006 <sup>*</sup>              | n = 11 (39%)  | 1.2                 | 0.8 – 1.8                               | 0.02                             | 0.3                                | CPLT   | 33                             | 1934                    | 0.5                          | B                                   | DN80ST                         |
|                           | HH007 <sup>°</sup>              | n = 0 (0%)  | -                   | -                                       | -                                | -                                  | -      | -                              | -                       | -                            | -                                   | -                              |
|                           | HH008                           | n = 6 (26%)   | 1.5                 | 0.4 – 6.4                               | 0.32                             | <1.3                               | INC    | -                              | 1934                    | -                            | C                                   | DN80ST                         |
|                           | HH009 <sup>×</sup>              | n = 9 (38%)   | 3.9                 | 1.5 – 9.8                               | 4.86                             | <3                                 | INC    | -                              | 1928                    | -                            | A1                                  | DN80ST                         |
|                           | HH010                           | n = 3 (38%)   | 1.6                 | 0.2 – 13.7                              | 0.51                             | <0.7                               | INC    | -                              | 1937                    | -                            | C                                   | DN200ST                        |
|                           | HH011 <sup>^</sup> <sup>×</sup> | n = 4 (50%)   | 1.9                 | 0.2 – 18.6                              | 0.37                             | -                                  | -      | 150                            | 1963                    | 15                           | A1                                  | DN300ST                        |
|                           | HH012 <sup>°</sup>              | n = 0 (0%)  | -                   | -                                       | -                                | -                                  | -      | -                              | -                       | -                            | -                                   | -                              |
|                           | HH013 <sup>^</sup>              | n = 2 (40%)   | 1.8                 | -                                       | -                                | -                                  | -      | 65                             | 1939                    | 5                            | A1                                  | DN80ST                         |
|                           | HH014                           | n = 24 (55%)  | 1.6                 | 1.1 – 2.5                               | 1.41                             | -                                  | -      | 65                             | 1950                    | 5                            | A1                                  | DN100ST                        |
|                           | HH015                           | n = 1 (50%)   | 1.0                 | -                                       | 0.38                             | <0.9                               | INC    | 19                             | 1935                    | 1                            | A1                                  | DN80ST                         |
| Reported by the LDC       | HH100                           | n = 1 (13%)   | 0.7                 | -                                       | 0.14                             | -                                  | -      | -                              | 1994                    | -                            | C                                   | d225Pe                         |
|                           | HH101                           | n = 0 (0%)  | -                   | -                                       | 0.07                             | <0.7                               | INC    | -                              | 1960                    | -                            | C                                   | DN80ST                         |
|                           | HH102                           | n = 0 (0%)  | -                   | -                                       | 0.01                             | -                                  | -      | -                              | 1928                    | -                            | C                                   | DN125ST                        |
|                           | HH103                           | n = 0 (0%)  | -                   | -                                       | 0.03                             | -                                  | -      | -                              | 1963                    | -                            | B                                   | DN150ST                        |
|                           | HH104                           | n = 0 (0%)  | -                   | -                                       | -                                | -                                  | -      | -                              | 1930                    | -                            | C                                   | DN100ST                        |

451 <sup>+</sup> The LDC reported three leak locations, ≈ 30 m distance between the two ends, for this  
 452 location: two leaks with area of 5 cm<sup>2</sup> and one leak with area of 1 cm<sup>2</sup>

453 <sup>\*</sup> Complete measurements for the suction method and used for averaging

454 <sup>^</sup> Leak size reported as sum of total hole area of all the leaks on the pipeline

455 <sup>×</sup> Large difference between leak location and the tracer release location

456 <sup>°</sup> The LDC did not confirm a gas leak

457  
458  
459

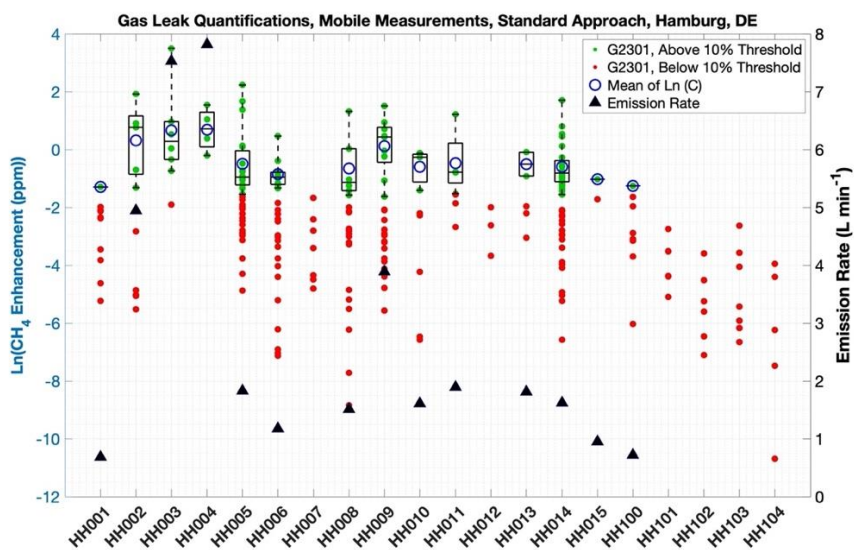
# Pipeline materials, steel (ST) or Polyethylene (Pe), pipeline Diameter Nominal (DN), which is close to the inner pipeline diameter in mm

### 3.2.1 Mobile method

461 The mobile method was applied at all the 20 locations (18 confirmed and 2 unconfirmed gas  
462 leak locations). At 14 (all confirmed gas leak locations) out of the 20 locations, CH<sub>4</sub>  
463 enhancements above the 10% threshold were observed and could be evaluated with the  
464 standard algorithm. The emission rate estimates for these 14 gas leak locations ranged from 0.7  
465 to 7.8 L min<sup>-1</sup>. At the 6 other locations we didn't observe any CH<sub>4</sub> enhancements above the  
466 10% threshold. When we lowered the enhancement threshold to 10 ppb, the emission rates  
467 were 0.07 (HH007; not confirmed gas leak location), 0.1 (HH012; not confirmed gas leak  
468 location), 0.04 (HH101), 0.02 (HH102), 0.05 (HH103) and 0.02 L min<sup>-1</sup> (HH104). Of the 5  
469 leak locations reported by the LDC, 4 did not show any enhancement maximum above the 10%  
470 threshold, i.e., these locations would not have been identified with the default algorithm  
471 (Weller et al., 2018) and would thus not produce an emission estimate.

472 Fig. 2 shows a summary of all individual observed enhancement maxima with the G2301  
473 analyzer from all transects with the mobile vehicle, which were used for the quantification of  
474 emission rates with Eq. 1. The figure illustrates the large spread in enhancement maxima for  
475 multiple passes at each location, similar to Luetschwager et al (2019), leading to large  
476 uncertainties in emission estimates of individual locations. Fig. 2 also shows the diversity of  
477 the various locations, where at some locations most or all of the observed enhancement maxima  
478 are above the 10% threshold (e.g. HH003 and HH004), at several locations none of the  
479 enhancement maxima was above the threshold (e.g. HH101 and HH104) and at other locations  
480 many transects showed enhancement maxima both above and below the threshold (e.g. HH006,  
481 HH008, HH009, HH014).

482 As shown in Fig. 3, there is a wide range of CH<sub>4</sub> enhancement observations per location. This  
483 depends on wind conditions, distance of the observed plume maximum to the emission outlet  
484 location, the superposition of emissions from several outlets and likely other variables such as  
485 soil water content. The mean relative uncertainty from the mean emission rate values for the  
486 mobile method is ≈ 70% for lower and 400% for the upper ends for the locations with at least  
487 3 transects (n = 10) which pass the 10% enhancement threshold (significant signals) in this  
488 study. The lower and upper ranges go down to 60% and 275% for the locations with at least 5  
489 transects (n = 7) with significant CH<sub>4</sub> enhancements.



490  
491  
492

Figure 3 – CH<sub>4</sub> enhancement maxima from all individual transects for each location using G2301. Red points show CH<sub>4</sub> enhancement maxima below the 10% threshold, green

493 **points show CH<sub>4</sub> enhancement maxima above the 10% threshold, thus used for the**  
494 **standard quantification. Blue circles show the  $\ln(C_{max})$  of all the green points for each**  
495 **location, and black triangles show the derived mean emission rate (based on all green**  
496 **points) using Eq. 1 for the location with at least one green point (right y-axis).**

497

### 498 **3.2.2 Tracer method**

499 The tracer method performed emission rate quantification at 16 gas locations out of 20  
500 locations. The derived emission rates range from 0.03 to 5.3 L min<sup>-1</sup> (Table 1). For 4 locations  
501 the tracer method was not applied because (i) the emissions were not persistently observable  
502 and the LDC also didn't confirm existence of gas leaks at these locations (n = 2; HH007 and  
503 HH012) or (ii) the leak had already been repaired (n = 1; HH013) or (iii) no emission was  
504 detectable during the visit of the tracer team (n = 1; HH104). For two of the locations (HH11  
505 and HH09), where leaks were confirmed and the tracer method was successfully deployed,  
506 later investigations during repair actions (see Fig. 1) showed that the surface emission outlets  
507 were located far (15 to 60 m) from the actual gas pipeline leak location indicating underground  
508 gas migration. It is evident from Table 2 that the tracer technique can also quantify very small  
509 emission rates, below the cut-off of the mobile technique of 0.5 L min<sup>-1</sup>. Emission rate  
510 estimates derived from the tracer technique were in general lower than the ones derived from  
511 the mobile technique, except for three sites where they were comparable (HH004, HH009 and  
512 H014).

513

### 514 **3.2.3 Suction method**

515 Due to the time-consuming nature of the suction measurements, initially 10 gas leak locations  
516 had been planned for deployment of the suction method in this campaign. The goal was to  
517 cover a wide range of expected emission rates, as stated in the intercomparison matrix. The  
518 suction method was applied at 8 gas leak locations (see Table 1) out of which the suction  
519 quantification was complete (HH006) according to protocol where an equilibrium  
520 concentration has to be reached. This was at HH006, with a derived emission rate of 0.3 L min<sup>-1</sup>.  
521 At several of the locations where the mobile method had indicated high emission rates,  
522 subsurface accumulation was widespread, and the suction method was either not deployed (n  
523 = 3; HH003, HH04, HH011) or the measurements were incomplete (n = 7; HH001, HH002,  
524 HH008, HH009, HH010, HH015 and HH101) because of either safety reasons or because the  
525 suction team estimated that they would be unable to complete the measurements within a day.  
526 For the 7 locations with incomplete suction measurements, the emission rates were reported  
527 ranging from 0.7 to 3 L min<sup>-1</sup>. These can be regarded as upper limit estimates because suction  
528 was not yet completed and CH<sub>4</sub> concentrations would have supposedly dropped further.

529

### 530 **3.2.4 Hole method**

531 For 5 locations where the leak area of a single gas pipeline leak was reported, the corresponding  
532 emission rates are between 19 to 65 L min<sup>-1</sup>. For locations HH011 and HH013, the hole area  
533 was reported as the sum of several holes and the total hole area for these two locations resulted  
534 in an emission rate of 150 and 65 L min<sup>-1</sup>, respectively. The quantification from the hole method  
535 is higher than from the mobile, tracer and suction methods by at least an order of magnitude.

536

### 537 **3.3 Leak categories**

538 The 20 (18 confirmed + 2 not confirmed) locations can be divided into four main categories  
539 related to measurement challenges of the various methods. These categories may overlap.

- 540 (i) Large subsurface CH<sub>4</sub> accumulation
- 541 (ii) Insufficient CH<sub>4</sub> enhancements for mobile quantification
- 542 (iii) Large CH<sub>4</sub> enhancement variability for mobile quantification

543 (iv) Several outlets and / or leaks or atmospheric turbulence

544 In this section we present the overall results and discuss in detail one selected location for each  
545 of these categories. The remaining locations (with similar characteristics) are presented in the  
546 SI.

547

### 548 **3.3.1 Location type I – Large subsurface CH<sub>4</sub> accumulation and multiple outlets**

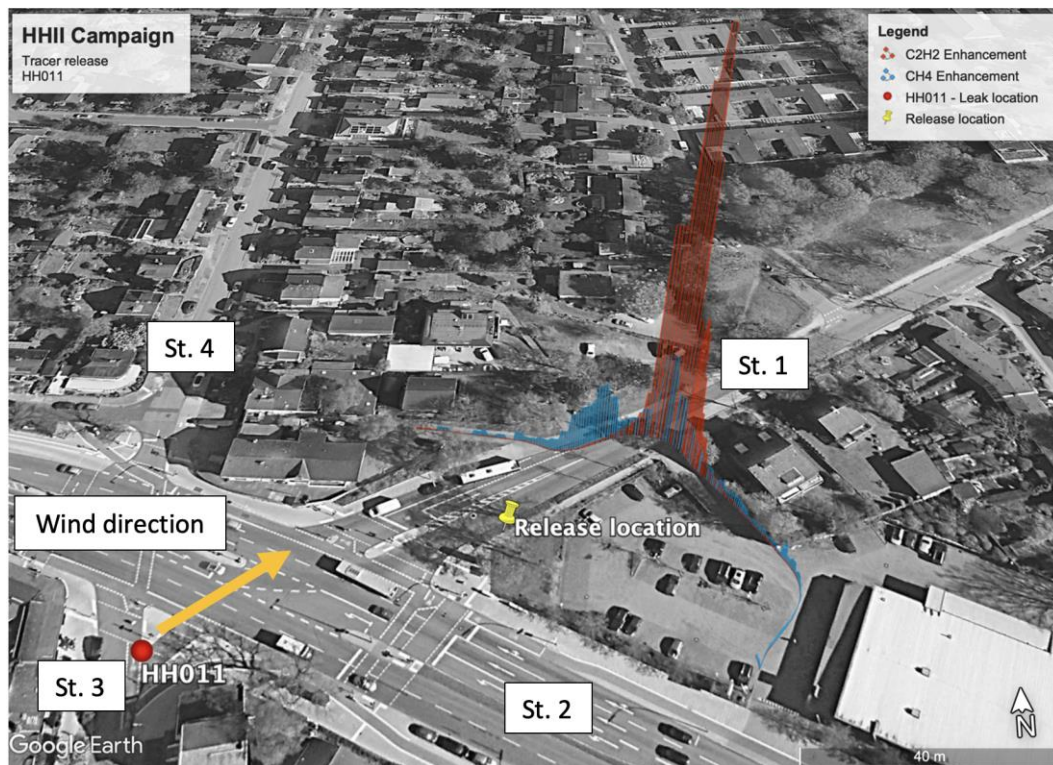
549 The spatial spread of surface emission outlet locations identified with the G4302 instrument as  
550 part of the mobile method provides an indicator for the extent of the subsurface accumulation  
551 of CH<sub>4</sub>. For 5 locations, emission outlets were found at great distance from each other, in order  
552 of tens of meters. The total emission of a gas leak is equal to the sum of emissions from all the  
553 surface outlets at a location, thus it is necessary to quantify each outlet separately to get the  
554 total emission.

555 HH011 (Fig. 4) is an example where very widespread CH<sub>4</sub> accumulation and migration was  
556 observed. During the initial mobile gas leak detection, leaks were located at the intersection of  
557 streets 1 and 2, close to a subsurface vent and a rain drain,  $\approx 2$  m far apart, (the yellow pin in  
558 Fig. 4a) based on clear signals from these outlets and a sign next to the road indicating presence  
559 of gas pipelines. The vent showed a C<sub>2</sub>:C<sub>1</sub> ratio of 2% (R<sup>2</sup> of 0.8 and max CH<sub>4</sub> mole fraction  
560 of 31 ppm) and we observed C<sub>2</sub>:C<sub>1</sub> ratio of 2.8% with R<sup>2</sup> of 0.96 and max CH<sub>4</sub> mole fraction  
561 of  $\approx 70$  ppm from the rain drain, clearly indicating a large / dominant contribution from fossil  
562 CH<sub>4</sub>. However, after quantifying the emission from these two leaks using the mobile and the  
563 tracer release methods, the LDC found the actual gas pipeline leak, during the repair actions,  
564 on the south side of the intersection, far from the vent and the rain drain, at the intersection of  
565 street no. 3 and no. 2 indicating that the gas had travelled about 60 m underground. It is possible  
566 that the leak resulted in several gas emission outlets, likely closer to the gas pipeline leak  
567 location. The emission rate measured using the mobile method was 1.6 L min<sup>-1</sup> based on 5  
568 plume transects and is likely underestimated because some emission outlets potentially were  
569 not included in the performed plume transect. It should also be noted that the distance from the  
570 gas pipeline leak location to the plume transect is larger than the distances applied during the  
571 controlled release calibrations (average 15 m) (Weller et al., 2019).

572 The tracer was released at the vent and the rain drain and thus measured the combined emission  
573 from these two outlets to be 0.4 L min<sup>-1</sup>. If the gas pipeline leak gave rise to multiple  
574 unidentified surface emission outlets, the emission from the gas pipeline is underestimated. IN  
575 fact, Fig. 4b shows that a CH<sub>4</sub> plume without C<sub>2</sub>H<sub>2</sub> was observed during the tracer release  
576 measurements at HH011, confirming that at least one other source of methane emission was  
577 present nearby.

578 Based on the previous experience at locations with widespread subsurface accumulation it was  
579 concluded that the suction method could not be applied at this location. The other case in this  
580 category was HH009.





581  
 582 **Figure 4 – aerial image of HH011 (© Google Maps). A gas leak location with widespread**  
 583 **undersurface CH<sub>4</sub> accumulation. The yellow pin shows the assumed leak location and**  
 584 **location of tracer release, which was very different from the actual leak location as**  
 585 **identified by the LDC (red circle). St. 1-4 are added to identify streets that are discussed**  
 586 **in the text. General wind direction during tracer release deployment is shown with an**  
 587 **orange arrow. CH<sub>4</sub> (in blue) and C<sub>2</sub>H<sub>2</sub> (in red) levels measured at a plume transect. One**  
 588 **of the CH<sub>4</sub> plume is proportional to the C<sub>2</sub>H<sub>2</sub> plume while the other CH<sub>4</sub> plume lacks the**  
 589 **C<sub>2</sub>H<sub>2</sub> signals suggesting existence of at least another emission outlet.**

590  
 591 The LDC reported the total area of several holes in the pipeline as 15 cm<sup>2</sup> for HH011, which is  
 592 the largest leak size among all the locations. If we assume that there was one hole with this  
 593 size, then the emission rate estimated by Eq. 3 will be 150 L min<sup>-1</sup>, a hole of 5 cm<sup>2</sup> gives  
 594 emission rate of 65 L min<sup>-1</sup>. The pipeline for this location was DN300ST and has been in  
 595 operation since 1963.

596  
 597 **3.3.2 Location type II – Insufficient CH<sub>4</sub> enhancements for mobile quantification**

598 At HH101, on a narrow ( $\approx 3$  m wide) street, which had about 1 m wide bare soil pavement on  
 599 one side, the LDC reported a gas leak location based on their routine surveys. On both sides of  
 600 the street there were about  $\approx 1.5$  m tall bushes and some trees. All three methods (mobile, tracer  
 601 and suction method) were deployed at this location. Gas emissions found their way to the  
 602 atmosphere through cracks in the asphalt with C<sub>2</sub>:C<sub>1</sub> ratio of 2.5% (R<sup>2</sup> of 0.93) with max CH<sub>4</sub>  
 603 mole fraction of  $\approx 25$  ppm. None of the CH<sub>4</sub> enhancement maxima observed during the mobile  
 604 surveys at this location were above the 10% enhancement threshold with the G2301 instrument,  
 605 thus this location would not be labeled as LI and no quantification would be reported from  
 606 mobile method as implemented in Weller et al (2019) and Maazallahi et al. (2020). The tracer  
 607 method was applied in static mode at a distance of  $\approx 15$  m and reported an emission rate of 0.1  
 608 L min<sup>-1</sup>, which is compatible with the emission strength being below the “detection limit”  
 609 defined by the 10% cut-off of the standard algorithm (0.5 L min<sup>-1</sup>). When the emission strength  
 610 is evaluated using the CH<sub>4</sub> enhancements below the cut-off, the value is 0.04 L min<sup>-1</sup>. The

611 suction method was applied at this location but an equilibrium was not achieved after 9 hr, i.e.  
612 incomplete suction measurements, and an upper limit for the emission rate of  $\approx 0.7 \text{ L min}^{-1}$  was  
613 reported. The fact that the suction measurement was incomplete at this location with a small  
614 emission rate shows that subsurface accumulation can also be large for smaller leaks.

615 Three of the leak locations in this study only showed one  $\text{CH}_4$  enhancement above threshold.  
616 The 10% threshold is a constraint, which removes enhancements less than about 200 ppb. This  
617 means for the locations where we only have one transect with  $\text{CH}_4$  enhancements more than  
618 the 10% threshold, the minimum emission rate estimated is about  $0.5 \text{ L min}^{-1}$ , no matter how  
619 many transects we had with  $\text{CH}_4$  enhancements less than the 10% threshold. This situation was  
620 observed for HH001, HH015 and HH100 (Fig. 5). In this case, the mobile method likely  
621 overestimates the total leak rate, because only the maximum enhancement is used for  
622 quantification. The tracer method reported low emission rates for these three sites  $0.12 \text{ L min}^{-1}$   
623 on average ( $n = 6$ ).

624 For the two locations (HH007 and HH012) where the LDC didn't confirm gas leaks (despite  
625 periodic observation of  $\text{C}_2\text{H}_6$  at outlets during the mobile surveys) none of the transects showed  
626  $\text{CH}_4$  enhancement maxima above the 10% threshold. At HH007, the outlet was through cracks  
627 in the pavement but at HH012 the outlets were from manholes. At HH007 the outlet location  
628 had shifted by about 2 m for two different days (4-week gap). We note that the correlation  
629 coefficients between  $\text{CH}_4$  and  $\text{C}_2\text{H}_6$  at these locations were between 0.4 and 0.6, so less than  
630 0.7, which is the threshold correlation we accepted for the outlets. As a leak was not confirmed  
631 for these locations, the tracer and suction methods were not applied.

632

### 633 **3.3.3 Location type III – Large $\text{CH}_4$ enhancement variability for mobile quantification**

634 For several locations, we observed a large variability of  $\text{CH}_4$  enhancements from different  
635 transects. One example is HH008, where only 6 of the 23 transects exceeded the 10% threshold,  
636 i.e. the leak was only observed in about every 4<sup>th</sup> transect. The leak location of HH008 is an  
637 example where  $\text{CH}_4$  enhancements from several transects cover a wide range. Based on the 6  
638 transects, which showed enhancement maxima above the 10% threshold, a leak rate of  $1.5 \text{ L}$   
639  $\text{min}^{-1}$  is derived. This may be an overestimate since many transects with maxima below the  
640 threshold were not considered. For this location the mobile tracer method was applied, which  
641 resulted in a leak rate quantification of  $0.3 \text{ L min}^{-1}$ .

642 The suction method derived an upper emission estimate of  $1.3 \text{ L min}^{-1}$  from incomplete  
643 measurements at HH008. The LDC reported a C category leak for this location from a DN80ST  
644 pipeline, which was installed in 1934.

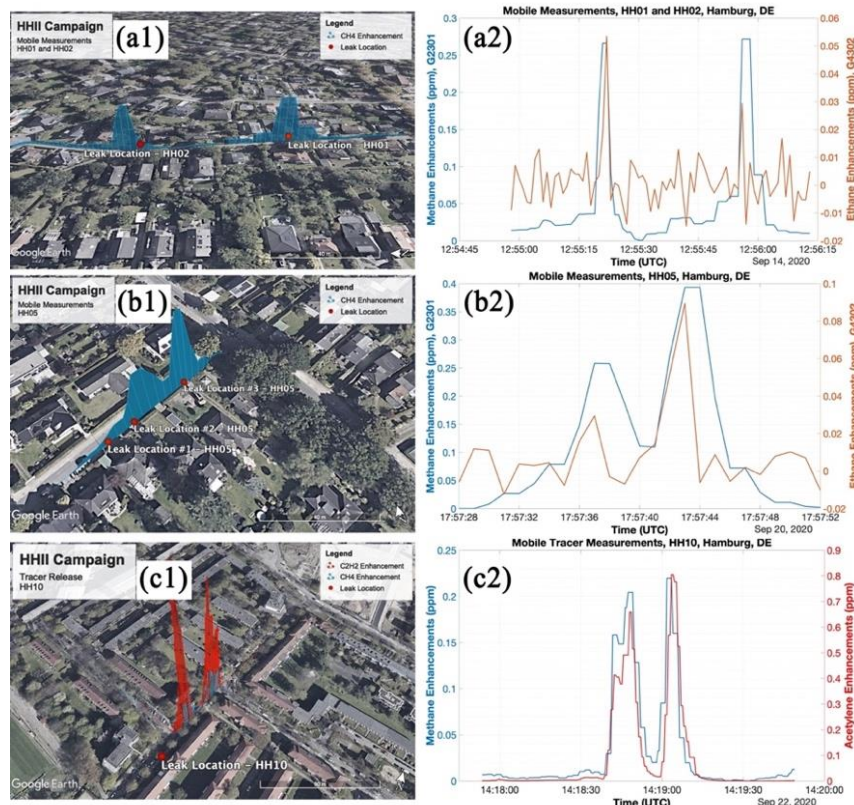
645

### 646 **3.3.4 Location type IV – Several outlets and / or leaks or atmospheric turbulence**

647 On a  $\approx 5 \text{ m}$  wide street, we detected two leaks about 80 m away from each other, HH001 and  
648 HH002 (Fig. 5a). It was a cobblestone street and there were bushes and few trees planted,  
649 mostly on one side of the street. The mobile method performed 10 transects at both locations  
650 and all the transects were accepted for the evaluation. The tracer team could quantify both  
651 locations using static measurements. The suction team began to quantify HH002 and HH001,  
652 but during quantification of HH001, there was a small accident (fire due to contact of drilling  
653 head with electric cable) and the leak had to be fixed immediately. The plumes on this street  
654 were sufficiently separated to positively identify two different leaks on the same street. In  
655 contrast, at location HH005, we observed several maxima for the same transect, but because  
656 the maxima were close to each other, those were clustered together in the mobile measurement  
657 algorithm (Fig. 5b). Later the LDC reported even three individual pipeline leaks on this street.  
658 In another example (HH010), some transects showed several plume maxima although only one  
659 emission outlet and later on only one gas pipeline leak was found (Fig. 5c). However, the  
660 release of the tracer resulted in several matching  $\text{CH}_4$  and tracer gas plumes confirming that



661 the emission indeed occurred from a single outlet and that the multiple plumes at this location  
 662 were due to inhomogeneous plume dispersion. This illustrates that the existence of several  
 663 maxima in one transect does not necessarily correspond to presence of several leaks and/or  
 664 outlets, but it can also be related to a spatially heterogeneous/disturbed plume. This shows that  
 665 the signals from the mobile detection method are not sufficient to allow determining the  
 666 number of leaks at a location with several plume at a close distance from each other in a single  
 667 transect.  
 668



669 **Figure 5 - several maxima observed during a single transect on one street showing**  
 670 **different situations: two well isolated leaks with about 80 m distance from each other (a1**  
 671 **and a2, HH001 and HH002), three pipeline leaks close to each other with several emission**  
 672 **outlets (b1 and b2, HH005) and one leak and one outlet but several CH<sub>4</sub> enhancement**  
 673 **maxima due to turbulence (c1 and c2, HH10), aerial images: © Google Maps.**  
 674  
 675

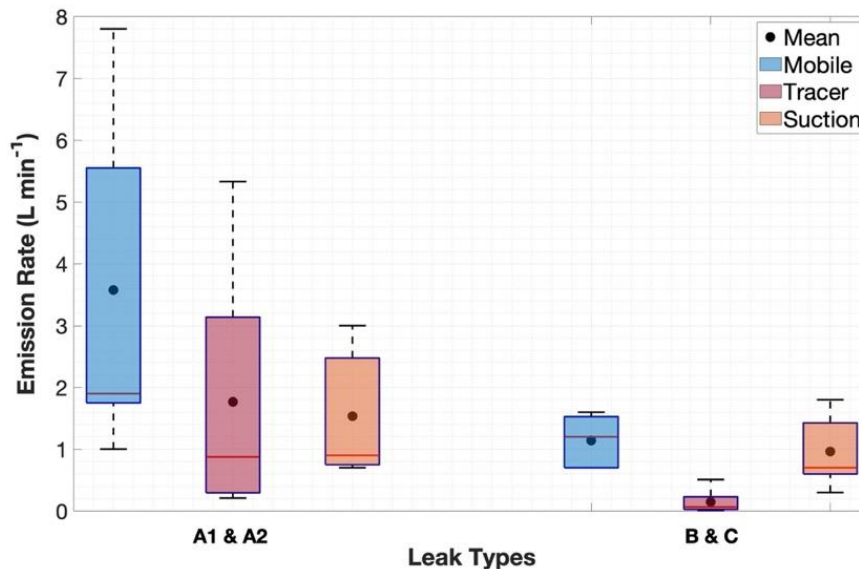
676 After detection by mobile measurements, emissions out of the ground were detected at HH001  
 677 and HH002 with the G4302 backpack within 3 m distance from the gas pipeline leak locations,  
 678 which was later reported by the LDC. For the single transect with a maximum above the 10%  
 679 threshold observed with the mobile method, the derived emission rate at HH001 was 0.8 L min<sup>-1</sup>  
 680 (n = 1). For HH002, the derived emission estimate for the transects with maxima above the  
 681 threshold is 5.2 L min<sup>-1</sup> (n = 5) from the mobile method. At HH002, individual derivation of  
 682 emission from separate CH<sub>4</sub> enhancement gives a wide range between 0.7 and 36.0 L min<sup>-1</sup>  
 683 (95% confidence) from the mobile method (see category III above). For HH001, the tracer  
 684 method was applied in static mode at ≈ 30 m distance to the release point and ≈ 40 m far from  
 685 HH002. The derived emission rate for HH001 is 0.06 L min<sup>-1</sup> and for HH002 0.22 L min<sup>-1</sup> from  
 686 the tracer method. For HH001, after about 5 hr of pumping, the suction quantification had to  
 687 be stopped due to the incident described above. Based on the incomplete suction measurement  
 688 an upper limit for emission rate of ≈ 1.8 L min<sup>-1</sup> for HH01 was estimated. An emission estimate  
 689 of ≈ 0.7 L min<sup>-1</sup> was derived for HH002 from an incomplete suction measurement. The LDC

690 reported leak size of  $\approx 2.5 \text{ cm}^2$  for HH001 and for  $\approx 3 \text{ cm}^2$  for HH002 which then give emission  
 691 rate of 39 and 45  $\text{L min}^{-1}$  respectively from the hole method. For both locations, leaks were due  
 692 to pipeline corrosion.

693

### 694 3.4 Emission rates of different leak safety types

695 The 18 confirmed gas leak locations that were investigated in the campaign were categorized  
 696 into the four safety categories, A1 (n = 7), A2 (n = 2), B (n = 2) and C (n = 7). The mobile  
 697 method quantified all the A1 and A2 leaks (n = 9) with an average emission rate of 3.6  $\text{L min}^{-1}$ .  
 698 5 out of 9 leaks in categories of B and C leaks were quantified with the mobile technique  
 699 including the 10% threshold with average emission rate of 1.1  $\text{L min}^{-1}$  (n = 5). Apart from one  
 700 location, which had to be fixed before the measurements, the tracer method quantified the A1  
 701 and A2 leaks (n = 8) and reported an average emission rate of 1.8  $\text{L min}^{-1}$ . The tracer method  
 702 also quantified all the B and C leaks (n = 9) with an average emission rate of 0.1  $\text{L min}^{-1}$ .  
 703 Mostly due to the safety and time constraints and medium to large underground accumulations  
 704 of  $\text{CH}_4$ , the suction method could provide incomplete measurements at only 3 locations of A1  
 705 and A2 leaks with an average emission rate of 1.5  $\text{L min}^{-1}$  (n = 3). The suction method measured  
 706 at 5 out of 9 B and C locations, one of the measurements was complete and the others were  
 707 incomplete, with an average emission rate of 1.0  $\text{L min}^{-1}$  (n = 5). Although the number of  
 708 quantified leaks is limited, all the three methods show that the emission rates from category A1  
 709 and A2 leaks are higher than category B and C leaks (Fig. 6). This indicates that the site  
 710 selection bias of measurements for the suction method due to safety concerns (see qualifier  
 711 above), can lead to a bias in the emission rate in this method.



712

713 **Figure 6 – Emission rate differences between different gas leak categories**

## 714 4 Discussion

### 715 4.1 Leak detection methods

#### 716 4.1.1 Leak location vs outlet location

717 There is a difference between the location of the leak in the gas pipeline (leak location; See  
 718 Sect. S.7 in SI) and the location where the gas is emitted to the atmosphere (outlet locations;  
 719 See Sect. S.2 in SI). Furthermore, a single leak in the gas pipeline can result in multiple  
 720 emission outlets at the surface. In this campaign we observed that in most cases (2 out of 18),  
 721 the emission outlet at the surface occurred only a few m (sometimes < 1 m) from the location  
 722 of the leak in the gas pipeline. However, in one case, an emission outlet was detected about 60

723 m away from the leak location indicating significant underground gas accumulation and  
724 migration (see Fig. 4).

725

#### 726 **4.1.2 Intercomparison of the gas leak detection methods**

727 The mobile method detects atmospheric CH<sub>4</sub> enhancements while measuring continuously with  
728 ppb precision from an inlet installed at the front bumper of the car while LDCs apply the carpet  
729 method with an instrument precision at the ppm level. High precision for the carpet method is  
730 not needed as the inlet to their instruments is connected to a carpet, which is attached to the  
731 ground. The mobile method can cover larger areas in shorter times, but not all roads, walkways,  
732 or other surface areas where pipelines are buried are accessible with a vehicle. The advantage  
733 of the carpet method is that it can precisely follow the pipeline map, which also means that it  
734 can locate leaks more precisely. The mobile method use a 10% threshold to neglect unreliable  
735 gas leak sources, which sometimes results in neglecting actual signals from small leaks. Also  
736 the mobile measurements do not detect all leaks due to the dependence on the wind direction  
737 (only downwind sources leaks can be detected). Luetschwager et al. (2021) suggested that 5 to  
738 8 plume transects give > 90% probability of gas leak detection at a given location, so if all the  
739 streets in an urban area are covered 5 to 8 times, > 90% of the leaks can be detected by mobile  
740 measurements.

741 Both the mobile and the carpet method use C<sub>2</sub>H<sub>6</sub> signals for distinguishing between fossil and  
742 microbial CH<sub>4</sub> emissions, and as for C<sub>2</sub>H<sub>6</sub>, the instrument used in the mobile method is more  
743 sensitive, and faster. In the carpet method, the laboratory analysis of C<sub>2</sub>H<sub>6</sub> is slow and with  
744 higher detection threshold compared to the mobile method, where C<sub>2</sub>H<sub>6</sub> is measured in real-  
745 time during the surveys, and also on foot from the emission outlet. The CRDS instrument  
746 provides real-time measurements of CH<sub>4</sub> and C<sub>2</sub>H<sub>6</sub> at 1 Hz frequency so checking various  
747 outlets at a possible gas leak location is faster.

748 At 14 out of the 20 locations in this study, gas leaks were detected (CH<sub>4</sub> signals passing the  
749 10% threshold) and quantified with the mobile method. However, we observed that 4 out of 5  
750 locations reported by the LDC would not have been detected in mobile surveys without prior  
751 information on existence of the leaks because the maximum enhancement was below the  
752 mobile detection threshold. At the only location (HH100) from the list of the LDC, where  
753 mobile method could quantify the emissions, the outlets were located on the road and the  
754 vehicle was driving on top of the outlet. For this location only one of the transects passed the  
755 10% enhancement threshold, and the quantification for this location was  $\approx 0.7 \text{ L min}^{-1}$ , close  
756 to the detection threshold of this method,  $\approx 0.5 \text{ L min}^{-1}$ . One of the other locations, HH101,  
757 reported by the LDC had similar surrounding conditions (e.g. presence of buildings, road  
758 conditions, etc.) as the other leaks detected by the mobile method, but still the mobile method  
759 was not able to detect a gas leak at this location without a priori information from the utility.  
760 The quantifications made by the tracer method suggest that the emission rates of the locations  
761 provided by the LDC were much lower than the locations detected by mobile measurements  
762 (Table 2). The 10% threshold in the mobile method precludes the identification of small leaks  
763 ( $< 0.5 \text{ L min}^{-1}$ ), which would only be identified by the carpet method.

764

## 765 **4.2 Signal attribution in mobile detection method**

### 766 **4.2.1 Attribution during mobile survey in car**

767 During the mobile measurements we used two approaches to find correlation between CH<sub>4</sub> and  
768 C<sub>2</sub>H<sub>6</sub>. When we compare the online measurements point by point, the probability of detecting  
769 a fossil signal is high, as only one single significant reading is sufficient to indicate a fossil  
770 signal. When we use the R<sup>2</sup> of the linear correlation between CH<sub>4</sub> and C<sub>2</sub>H<sub>6</sub> enhancements  
771 above the cut-off, the attribution is more reliable. In a large dataset without a priori information

772 on the existence of a gas leak at different locations, the correlation method is more trustworthy  
773 as the point-by-point method could be affected by instrument noise and/or spikes.  
774 We also used CO<sub>2</sub> signals and their correlation with CH<sub>4</sub> signals to investigate interference  
775 from combustion or microbial processes. For only 7 plumes at 6 locations, we detected  
776 correlations between CO<sub>2</sub> and CH<sub>4</sub>, which could indicate either oxidation of CH<sub>4</sub> to CO<sub>2</sub> or  
777 mixture of microbial CH<sub>4</sub> emissions from e.g. the sewer system with the emissions from natural  
778 gas leaks. The number of these possible co-emissions is low compared to the number of total  
779 transects (only  $\approx 7\%$  of the plumes with CH<sub>4</sub> enhancements greater than 10%), thus such an  
780 admixture of microbial CH<sub>4</sub> should not impact the quantification from mobile method  
781 significantly.

#### 782 **4.2.2 Plume attribution to emission outlets**

784 The outlet attribution was performed using the G4302 CRDS instrument which is portable like  
785 a backpack. We checked the outlets (See Sect. S.2, Fig. S1) around the locations of interest and  
786 evaluated the correlation between CH<sub>4</sub> and C<sub>2</sub>H<sub>6</sub> and the persistence of the emissions on  
787 different days. In theory, it is possible to estimate contributions of fossil and microbial CH<sub>4</sub> in  
788 a plume using the ethane signals during the mobile measurements with the vehicle and the  
789 reference C<sub>2</sub>:C<sub>1</sub> ratio provided by the LDC. However, due to the low C<sub>2</sub>H<sub>6</sub> signals in ambient  
790 air, it was not feasible to quantify the possible contribution of microbial methane emissions.  
791 Nevertheless, the C<sub>2</sub>H<sub>6</sub> signals of the G4302 CRDS instrument were still very useful to identify  
792 a location as a possible gas leak location or not. For all the 15 locations, which were initially  
793 detected by the mobile method we observed detectable C<sub>2</sub>H<sub>6</sub> signals, including the two  
794 locations which later were not confirmed as a gas leak location by the LDC. This suggests that  
795 either the leak is at a greater distance and depending on the transport of the emission we  
796 periodically can see the signals at the detected outlets or that there are sources that produce  
797 both CH<sub>4</sub> and C<sub>2</sub>H<sub>6</sub> in the vicinity of the location.

### 799 **4.3 Leak quantification methods**

#### 800 **4.3.1 Mobile method**

801 If the outlets are close to each other, we may observe several CH<sub>4</sub> enhancements close to each  
802 other or overlapping when a single transect is performed at a close distance. If we assume that  
803 the number of CH<sub>4</sub> maxima is equivalent to the number of real outlets that exist on a road and  
804 only use the maximum enhancements from the most pronounced plume to calculate the  
805 emission rate, the total emission will be underestimated with the mobile method.

806 Emission rate estimates with the mobile method from individual transects are associated with  
807 high uncertainty, related to variabilities in either above-ground or under-ground conditions. For  
808 example, an unfavorable wind direction (above ground condition) can result in missing a plume  
809 from a gas leak. The mobile measurement van itself may also affect the measurement, e.g., by  
810 creating pressure fluctuations. Luetschwager et al. (2021) showed that the quantifications from  
811 the same leak in individual mobile transects can vary by more than an order of magnitude. In  
812 Hamburg, we found that the range can be even a factor 50 or 100 in exceptional cases (Table  
813 2). This high variability illustrates that if we perform only one transect per location, the  
814 estimated leak emission rate can result in high under / overestimation in emission estimate for  
815 the single location, as was also reported by Maazallahi et al. (2020). This large uncertainty for  
816 individual locations is less severe when the results are extrapolated to the city-level, where the  
817 sample size is also large, including over- and underestimates (Brandt et al., 2016).

818 In our previous study in Hamburg (Maazallahi et al., 2020) the overall average emission rate  
819 for all the LIs was estimated  $3.4 \text{ L min}^{-1} \text{ LI}^{-1}$  ( $n = 145$ ) while for the fossil-attributed  
820 locations it was  $5.2 \text{ L min}^{-1} \text{ LI}^{-1}$  ( $n = 45$ ; standard error of 3.1). This showed that the biggest  
821 emitters were among the fossil categories. In the present study, the average emission rate from

822 mobile measurements for the gas leak locations is  $2.7 \text{ L min}^{-1} \text{ LI}^{-1}$  ( $n = 14$ ; standard error of  
823 0.6). The higher average emission rate per fossil location in the first campaign may have been  
824 caused by the fact that in that campaign only a smaller number of transects were performed per  
825 location (on average 1.1 in the previous study versus 6.9 transects with  $\text{CH}_4 > 10\%$  threshold  
826 per location in the present study). Luetschwager et al. (2021) stated that after 6 transects with  
827  $\text{CH}_4$  exceeding the 10% threshold per location the average overestimation of leak size estimates  
828 will be less than 10%. In addition, the differences in sample size and locations in these two  
829 studies (45 versus 14 locations in the first and second studies respectively) may partially  
830 explain the difference in average. This is because the probability of detecting large emitters,  
831 which increase the average emission rate of all leaks, increases with sample size.

832 The two  $\text{CH}_4$  sensors onboard the mobile van play specific roles in the detection and  
833 quantification of leaks.  $\text{CH}_4$  enhancements on the G2301 are 3.8 times lower than the G4302.  
834 This is an artefact of the G2301, which smoothes the signal compared to the G4302 because of  
835 the slower pump and sampling rate (See Sect. S.8.1 in SI). On the other hand, this results in  
836 more signals passing the 10% threshold on G4302. This then also leads to higher detection  
837 probabilities using G4302 (See Sect. S.8.2 in SI). Higher record of  $\text{CH}_4$  enhancements then  
838 also results in higher emission rate quantification using Eq. 1 (See Sect. S.8.3 in SI). We use  
839 the G2301 for quantification, since this is the instrument that was also used for introduction of  
840 the mobile equation quantification in Weller et al. (2017). The quantification of the gas leak  
841 locations using Eq. 1 depends only on the  $\text{CH}_4$  enhancements. This gives about a factor 2 higher  
842 emission rates from G4302 than from G2301 for the same plumes. When we evaluate the plume  
843 areas from the two instruments, they are much closer to the 1:1 line (See Sect. S.8.3 in SI). This  
844 agrees with findings from another study using two different in-situ instruments onboard a  
845 mobile car (See Sect. S1.5, Fig. S6 from Ars et al. (2020)). They also found that the plume area  
846 is closer to the 1:1 line in mobile measurements even if the air intakes are not at the same  
847 location of the vehicle. This suggests that the plume area is a more robust parameter than  
848 maximum enhancement for emission rate quantification and a leak rate quantification equation  
849 using the plume area should be developed.

850 In general, the closer the air intake is to the emission point the higher the  $\text{CH}_4$  mole fraction  
851 reading is (See Sect. S.9 in SI), but when several outlets are present at one location it is not  
852 possible to uniquely determine the distance to the emission point, and also determine which  
853 plume belongs to which outlet. Eq. 1 from Weller et al. (2019) only uses the maximum  $\text{CH}_4$   
854 enhancements above the 10% threshold from each pass. In their controlled release experiments  
855 the average distance between the leak and measurement was 15.75 m. Analysis of our results  
856 (Table S4, Sect S.5 in SI) shows that higher maximum concentrations are encountered more  
857 often when the distances of the transect to the leak location are small. For example, at HH002  
858 the transect was very close to the main emission point, which likely leads to the substantially  
859 higher emission rate estimate derived from the mobile method ( $4.9 \text{ L min}^{-1}$ ) compared to the  
860 tracer method ( $0.22 \text{ L min}^{-1}$ ). On the other hand, at HH011 the mobile method underestimates  
861 the emission rate (See Sect. 3.3.1), as at this location the measurement distance to the leak was  
862 larger than reference distance of 15.75 m applied by Weller et al. (2019). This suggests that to  
863 reduce the quantification error for individual leak locations, distance should also be included  
864 in an improved transfer equation.

865 The effect of neglecting or retaining the transects with enhancement maxima below the 10%  
866 threshold was quantitatively investigated for 5 locations where the tracer team conducted  
867 mobile measurements (See Sect. S.10 in SI). These measurements were evaluated as  
868 “controlled release” experiments for  $\text{C}_2\text{H}_2$ , because the actual  $\text{C}_2\text{H}_2$  release rate is known, and  
869 measurements were made in mobile mode. The standard mobile quantification algorithm with  
870 the 10% threshold yields emission estimates that are in relatively good agreement with the  
871 released quantities, whereas the estimates are biased considerably low when measurements

872 with maxima below the threshold are retained. This supports the use of the original method,  
873 which removes transects with an improper realization of the plume. Relating to section 4.5, it  
874 must be noted, however that in these measurements the distances of the C<sub>2</sub>H<sub>2</sub> maxima to the  
875 release points were between 30 to 45 m, thus larger than the normal distance of mobile CH<sub>4</sub>  
876 measurement to the emission outlets (from few meters up to 30 m).

877

#### 878 **4.3.2 Tracer method**

879 The tracer method is more labor intensive than the mobile method. However, the strength of  
880 the method is the application of a tracer gas providing the plume dilution and avoiding the use  
881 of atmospheric dispersion models and weather information. If the tracer release location does  
882 not reflect the sum of all the outlet emissions at a gas leak location, or misses some of the  
883 outlets, then the total emission quantification from the gas leaks will be underestimated. An  
884 example of such a case is site HH011 in this study where the leak location in the gas pipeline  
885 (after quantification; see Fig. 1) was found to be located about 60 m upwind the targeted  
886 emission outlet. During tracer quantification, an additional CH<sub>4</sub> plume (not defined by the  
887 tracer gas) was observed indicating more than one emission outlet (Fig. 4). The confirmation  
888 for this is the finding of gas leak location by the carpet method. The emission rate of the  
889 targeted emission source (the vent and the drain) is thus not representing the combined  
890 emission from the gas leak in the pipeline located 60 m upwind the emission source. Further  
891 surface screening and leak detection would have been needed to identify and quantify all  
892 emission outlets.

893

#### 894 **4.3.3 Suction method**

895 The suction method is the most labor-intensive quantification method. Following a strict, safety  
896 first, protocol the gas utilities fix leaks in the A1 safety category immediately upon detection  
897 and A2 leaks within a week. Given logistical constraints, the suction method therefore mainly  
898 or exclusively quantifies B or C leaks (50% of confirmed gas leak location in this study). We  
899 investigated whether such a site selection bias could lead to a bias in the average quantified  
900 emission rate in the inventory report. In this study, we observed that the leaks detected from  
901 the mobile methods were mostly in the A1 and A2 category and the biggest emitters (based on  
902 the mobile and tracer release measurements) had soil CH<sub>4</sub> accumulation of a magnitude that  
903 prevented successful application of the suction method. Further research is needed to identify  
904 the physical mechanism(s) to explain the observed correlation between A1 and A2 leaks and  
905 high emission rates. As a hypothesis, the presence of soil cavities associated with leak category  
906 A1 may result in higher permeability, i.e. lower underground resistance, which then leads to  
907 higher emission rate for the same pipeline hole size compared to locations with no cavity.

908 The suction method was intended to be deployed right before the repair actions. For some of  
909 these locations, the suction method was in operation for more than 10 hours, but due to the high  
910 soil CH<sub>4</sub> accumulation, the measurements were stopped and labeled as incomplete in this study.  
911 For the other locations with high soil CH<sub>4</sub> accumulation, the suction method was not attempted,  
912 given the expectation (based on experience at the incomplete locations) that completion of  
913 measurements for leak rate quantification at those locations was unlikely.

914

#### 915 **4.3.4 Hole method**

916 Based on the leak size, pipeline depth and overpressure, the average emission rate was  
917 estimated at 40 L min<sup>-1</sup> (n = 5). We note that these estimated should be regarded as upper limits  
918 since flow restrictions outside the pipe are not included. The emission range of individual gas  
919 leaks based on the hole method is between 19 to 150 L min<sup>-1</sup> for 1 cm<sup>2</sup> to 15 cm<sup>2</sup> hole sizes  
920 respectively, larger than any of the measurement-based quantification methods. This method  
921 requires information about the overpressure of the gas pipeline, depth of buried pipeline and



922 size of a leak and it does not include the information about soil properties, which can impact  
923 the emission rate.

924

#### 925 **4.3.5 Intercomparison of methods**

926 In this study, a reliable quantitative intercomparison of the three methods (mobile, tracer and  
927 suction methods) was attempted. A complete comparison of all three methods was possible at  
928 only one out of 20 locations (18 confirmed gas leak locations) because of the long time (>8-10  
929 hrs) needed for full equilibrium of the suction method, whereby emission rates for 7 out of the  
930 8 leaks quantified by the suction method were reported as maxima rather than absolute values  
931 (Table 1). At these 7 locations the emission was thus overestimated.

932 In total, the average CH<sub>4</sub> emissions from natural gas pipeline leaks for the same locations where  
933 we have quantifications from mobile and tracer methods (n = 13) are 2.8 and 1.2 L min<sup>-1</sup>  
934 respectively. The suction method could only be completed at one location. The average  
935 emission rate reported for all the locations from the suction method (high bias due to  
936 incomplete measurement) is 1.2 L min<sup>-1</sup> (n = 8).

937 The higher emission rates derived with the mobile method are in qualitative agreement with  
938 previous studies. Weller et al. (2018) compared quantifications from the mobile measurements  
939 described in von Fischer et al. (2017) with the tracer method and surface enclosure method in  
940 four US cities. They reported that mobile measurement estimates were  $\approx 2.3$  L min<sup>-1</sup> greater  
941 than the tracer method mean estimates of  $\approx 3.2$  L min<sup>-1</sup> (n = 59). This was attributed to the  
942 overestimation of small leaks (< 2.4 L min<sup>-1</sup>) in the mobile measurements method, which we  
943 have also discussed above for our dataset. In addition, performance of only a few transects at  
944 individual locations also lead to systematically high biased emission rate estimates for higher  
945 emission rates (Luetschwager et al., 2021). Indeed, at the locations where we only have one  
946 transects with CH<sub>4</sub> enhancements above the 10% threshold, there is an overestimation from  
947 mobile method compared to the tracer method. For example, at HH001 (n=1), HH015 (n=1)  
948 and HH100 (n=1) the mobile method estimated emissions of a factor 4 higher in comparison  
949 to the tracer method. The analysis of Luetschwager (2019) clearly shows that this high bias is  
950 reduced when numerous transects are performed. Therefore, we carried out multiple transects  
951 to reduce this systematic bias. We note that there are also large differences between the mobile  
952 and tracer methods, e.g. HH002 and HH006. We suspect that the very short gas leak location  
953 distance to the mobile driving transects can explain partially the difference. Moreover,  
954 existence of another leak in the category of A1 at the HH006 location which had to be fixed  
955 prior to the tracer method could explain the difference in emission rate magnitude at this  
956 location. Nevertheless, the limited number of transects and the 10% threshold can contribute  
957 to an overestimation of the average leak rate with the mobile method at an individual location.  
958 At the same time, however, the mobile method fails to detect leaks entirely when the leak outlet  
959 is located downwind of the mobile van. The fact that the mobile method misses downwind  
960 emissions constitutes a method specific factor towards biasing city-wide emissions low, which  
961 qualitatively counteracts the high bias above.

#### 962 **4.4 Possible suction method sampling bias with implications for emission inventories**

963 Following our communications with the emission inventory experts (personal communications  
964 with Christian Böttcher, 2022), we cannot fully reconstruct the methods that are used in the  
965 existing national inventory report to establish the emission factors due to lack of transparency.  
966 However, the German environmental agency (UBA) is considering to use the results of the  
967 recent large scale measurement campaign based on the suction method (MEEM, 2018) in future  
968 publications of the national emission inventory in Germany (Federal Environment Agency,  
969 2021). The utilities choose leak locations for application of the suction method where there are  
970 no safety concerns and/or immediate leak closure is compulsory. This implies that this method  
971 is not applied at locations of the A1 category, which demand immediate repair (P. 27 in MEEM,

972 2018). Due to logistic constraints and the time-consuming nature of the suction measurements,  
973 they are likely also not (or rarely) applied at locations in the A2 category, which require repair  
974 within a week. Thus, suction measurements have a location sampling bias towards leaks in the  
975 B and C category. This is supported by the fact that the leak locations that were contributed by  
976 the LDC to the intercomparison campaign were locations in the B and C category. This study  
977 investigated whether this location sampling bias could result in an emission rate bias, which  
978 could contribute to the fact that the suction method did not report leaks with emission rates as  
979 high as they have been reported by the mobile method in this study or during previous  
980 measurements in the same city (Maazallahi et al., 2020).

981 In this study, emission rates from A1 and A2 category leaks were larger compared to those  
982 from B and C category leaks (Figure 6). The emission rate differences vary by measurement  
983 method: a factor 2 for the mobile method (n = 9 for A1&A2, n = 4 for B&C), a factor 11 for  
984 the tracer method (n = 8 for A1&A2, n = 8 for B&C) and a factor 1.6 for the suction method  
985 (n=3 for A1&A2, n = 5 B&C). For the mobile method, there is a clear separation between the  
986 A1&A2 versus the B&C categories. The highest emission estimate for the B&C group  
987 (HH010) is similar to the lowest emission rate estimate for the A1&A2 group (HH014).  
988 Furthermore, HH011 in the A1 category was very likely biased low because of the wrongly  
989 assumed leak location.

990 For the tracer method, the difference between the two groups is largest, an order of magnitude,  
991 and we know that emissions are underestimated at least at one location of the A1 category  
992 (HH011). The uncertainty of the tracer method is much smaller than the difference between the  
993 two groups. The tracer method also illustrates that 4 of the 5 leaks that were contributed by the  
994 LDC to the intercomparison campaign were extremely small. If these would be representative  
995 for locations where the suction method is usually applied, it would indeed indicate a severe  
996 emission rate bias for the suction method, not because the measurements themselves are biased,  
997 but because locations with low emission rates are targeted with this method. In the  
998 intercomparison campaign, we attempted to apply the suction method also at locations of the  
999 A categories, but at 8 out of 9 locations from the A category, the suction measurements could  
1000 not be applied for safety reasons, or suction could not be completed, because of the widespread  
1001 subsurface accumulation (Table 2). At the other A location (HH014), the suction method could  
1002 not be applied as the ground had been already opened for the repair.  
1003

## 1004 **5 Conclusion**

1005  
1006 In summer 2020, we compared three gas leak rate quantification methods, namely the mobile,  
1007 tracer, and suction methods, in Hamburg, Germany. While the mobile and tracer methods have  
1008 been compared previously, this is the first peer-reviewed study that includes the suction  
1009 method, although suction measurements could not be completed in one day at most locations.  
1010 The mobile method can cover large areas in a short time, but some of the smaller leaks (< 0.5  
1011 L min<sup>-1</sup>) are not identified as a gas leak location due to the 10% enhancement threshold in the  
1012 standard mobile quantification algorithm. While the mobile method quantification algorithm is  
1013 designed to accurately report city-level total gas distribution leak rates (i.e., considering a large  
1014 sample size), it has large (known) uncertainties for individual leaks. The tracer method has a  
1015 smaller uncertainty, but it is labor intensive in comparison to the mobile method. On average,  
1016 CH<sub>4</sub> emissions from natural gas pipeline leaks were higher from mobile quantifications in  
1017 comparison to tracer quantifications. For many locations, we encountered several outlets and  
1018 with widespread underground gas accumulations. At one location, after deployment of the  
1019 mobile and the tracer quantification and during the repair actions, it was found out that the  
1020 actual leak in the gas pipeline was located  $\approx$  60 m away from the identified emission outlet



1021 indicating significant underground gas migration. It is possible that this leak had several  
1022 emission outlets that were not identified and the emission quantified from the single outlet is  
1023 thus not representative for the whole emission from this leak.

1024 The suction method has a low reported uncertainty, but it is even more labor and time intensive  
1025 than the tracer method. Due to the time and effort needed to plan and execute the measurements,  
1026 the suction method is likely never applied in routine operation at A1 or A2 safety category  
1027 leaks that mandate immediate or near-time repair. In our study, it was also not feasible to apply  
1028 the suction method at locations with large subsurface CH<sub>4</sub> accumulations. Our results thus  
1029 indicate a systematic difference between A1 and A2 (high emissions) versus B and C (low  
1030 emissions) category locations, and generally larger emission rates are inferred with the mobile  
1031 and tracer methods for sites with widespread subsurface accumulation.

1032 This study did not allow a direct, quantitative comparison of emission rates estimated with all  
1033 three different methods because of the inability to quantify the same leak locations with all  
1034 methods. However, this inability illuminates the importance of site selection for deriving  
1035 representative emission factors based on empirical measurements. Specifically, the results  
1036 suggest that a significant emission rate bias could exist for measurements that are carried out  
1037 with the suction method. Our results therefore stipulate that representative site selection  
1038 includes sampling at all leak safety categories (MEEM, 2018). Otherwise, this could lead to a  
1039 sampling and emission rate bias in the national inventory of gas leak CH<sub>4</sub> emission in Germany.

1040

1041 **Authors contributions:** TR, HM and SS conceived and designed the study. TR coordinated  
1042 the campaign in collaboration with DBI, Technical University of Denmark (DTU),  
1043 Environmental Defense Fund (EDF), E.On and Gasnetz Hamburg (GNH) teams. HM carried  
1044 out the mobile measurements, emission outlet attribution, performed the analyses of mobile  
1045 data and collectively with TR analyzed the intercomparison results. AD, CS and AMF  
1046 performed the tracer method and reported the emission rates from the tracer dataset.  
1047 HDvdG and TR made instruments and equipment available for the mobile method and CS  
1048 provided those for the tracer method. HM wrote the paper, and all co-authors supported the  
1049 interpretation of the results and contributed to improving the paper.

1050

1051 **Competing interests:** The authors declare that they have no conflict of interest.

1052

### 1053 **Acknowledgement**

1054 This study was carried out with the financial support from the Environmental Defense Fund.  
1055 Extra financial supports were provided by the H2020 Marie Skłodowska-Curie actions through  
1056 Methane goes Mobile – Measurements and Modelling project (MEMO<sup>2</sup>; [https://h2020-  
1057 memo2.eu/](https://h2020-memo2.eu/), last access: 20 April 2022), grant number 722479. In this study, Robertson  
1058 Foundation supported contribution of Stefan Schwietzke. We appreciate efforts from  
1059 Luise Westphal, Michael Dammann, Ralf Luy, Christian Feickert, Volker Krell, Turhan Ulas,  
1060 Dieter Bruhns and Sönke Graumann, from GasNetz Hamburg GmbH who facilitated this study  
1061 by hosting the teams, arranging and applying the carpet method leak detection and confirmation  
1062 procedures, making information on gas leaks and pipelines available for the data analysis and  
1063 applying leak repair protocols. We extend our appreciation to Andre Lennartz, Stefan Gollanek  
1064 and Dieter Wolf from E.On-for their contribution in the planning of the campaign, deploying  
1065 the suction method at the locations, and exchanging their knowledge and experiences from  
1066 their previous campaigns. We thank the team from DBI Gas and Environmental  
1067 Technologies GmbH Leipzig (DBI GUT Leipzig) including Charlotte Große, who contributed  
1068 in providing information for structuring the campaign planning.

1069

1070

# Reference:

- 1071
- 1072 Alvarez, R. A., Pacala, S. W., Winebrake, J. J., Chameides, W. L., Hamburg, S. P.: Greater  
1073 focus needed on methane leakage from natural gas infrastructure, PNAS, 109 (17)  
1074 6435-6440, <https://doi.org/10.1073/pnas.1202407109>, 2012.
- 1075 Ars, S., Vogel, F., Arrowsmith, C., Heerah, S., Knuckey, E., Lavoie, J., Lee, C., Mostafavi Pak,  
1076 N., Phillips, J. L., and Wunch, D., Investigation of the Spatial Distribution of Methane  
1077 Sources in the Greater Toronto Area Using Mobile Gas Monitoring Systems, Environ.  
1078 Sci. Technol., 54, 24, 15671–15679, <https://doi.org/10.1021/acs.est.0c05386>, 2020.
- 1079 Allwine G., Lamb B., Westberg H., Application of Atmospheric Tracer Techniques for  
1080 Determining Biogenic Hydrocarbon Fluxes from an Oak Forest. In: Hutchison B.A.,  
1081 Hicks B.B. (eds) The Forest-Atmosphere Interaction. Springer, Dordrecht.  
1082 [https://doi.org/10.1007/978-94-009-5305-5\\_23](https://doi.org/10.1007/978-94-009-5305-5_23), 1985.
- 1083 Arnaldos, J., Casal, J., Montiel, H., Sánchez-Carricondo, M., Vílchez, J.A., Design of a  
1084 computer tool for the evaluation of the consequences of accidental natural gas releases  
1085 in distribution pipes, Journal of Loss Prevention in the Process Industries,  
1086 [https://doi.org/10.1016/S0950-4230\(97\)00041-7](https://doi.org/10.1016/S0950-4230(97)00041-7), 1998.
- 1087 Bousquet, P., Ciais, P., Miller, J. B., Dlugokencky, E. J., Hauglustaine, D. A., Prigent, C., Van  
1088 der Werf, G. R., Peylin, P., Brunke, E. G., Carouge, C., Langenfelds, R. L., Lathière,  
1089 J., Papa, F., Ramonet, M., Schmidt, M., Steele, L. P., Tyler, S. C., White, J.,  
1090 Contribution of anthropogenic and natural sources to atmospheric methane variability.  
1091 Nature.; 443(7110):439-43. <https://doi.org/10.1038/nature05132>, 2006.
- 1092 Brandt, A. R., Heath, G. A., and Cooley, D., Methane Leaks from Natural Gas Systems Follow  
1093 Extreme Distributions, Environmental Science & Technology, 50 (22), 12512-12520,  
1094 <https://doi.org/10.1021/acs.est.6b04303>, 2016
- 1095 Cho, Y., Ulrich, B. A., Zimmerle, D. J., Smits, K. M., Estimating natural gas emissions from  
1096 underground pipelines using surface concentration measurements, Environmental  
1097 Pollution, <https://doi.org/10.1016/j.envpol.2020.115514>, 2020.
- 1098 Defratyka, S. M., Paris, J. D., Yver-Kwok, C., Fernandez, J. M., Korben, P., and Bousquet, P.,  
1099 Environmental Science & Technology Article ASAP,  
1100 <https://doi.org/10.1021/acs.est.1c00859>, 2021.
- 1101 Delre, A., Greenhouse gas emissions from wastewater treatment plants: measurements and  
1102 carbon footprint assessment, Ph.D. Thesis, Department of Environmental Engineering,  
1103 Technical University of Denmark (DTU), Copenhagen, Available at:  
1104 <https://orbit.dtu.dk/en/publications/greenhouse-gas-emissions-from-wastewater-treatment-plants-measure>  
1105 <https://orbit.dtu.dk/en/publications/greenhouse-gas-emissions-from-wastewater-treatment-plants-measure> (Last Accessed: 15 June 2021), 2018.
- 1106 DVGW: High-performing infrastructure, (2022). [online] Available from  
1107 <https://www.dvgw.de/english-pages/topics/safety-and-security/technical-safety-gas>,  
1108 (Last Accessed: 25 January 2022)
- 1109 DVGW: Technische Regel-Arbeitsblatt; DVGW G465-1 (A) (2019). [online] Available from:  
1110 [https://shop.wvgw.de/var/assets/leseprobe//510544\\_lp\\_G\\_465-1\\_2019\\_05.pdf](https://shop.wvgw.de/var/assets/leseprobe//510544_lp_G_465-1_2019_05.pdf). (Last  
1111 Accessed: 15 December 2021)
- 1112 Ebrahimi-Moghadam, A., Farzaneh-Gord, M., Arabkoohsar, A., Jabari Moghadam, A., CFD  
1113 analysis of natural gas emission from damaged pipelines: Correlation development for  
1114 leakage estimation, Cleaner Production, <https://doi.org/10.1016/j.jclepro.2018.07.127>,  
1115 2018.
- 1116 EC: EU strategy to reduce methane emissions available at: <https://eur-lex.europa.eu/legal-content/EN/TXT/?uri=CELEX%3A52020DC0663&qid=1644853088591>,  
1117 (last  
1118 access: 28 March 2022), 2020

1119 EIA, Carbon Dioxide Emissions Coefficients , available at:  
1120 [https://www.eia.gov/environment/emissions/co2\\_vol\\_mass.php](https://www.eia.gov/environment/emissions/co2_vol_mass.php), (last access:  
1121 28 March 2022), 2021.

1122 EPA, Methane emissions from the natural gas industry: underground pipelines,  
1123 [https://www.epa.gov/sites/production/files/2016-08/documents/9\\_underground.pdf](https://www.epa.gov/sites/production/files/2016-08/documents/9_underground.pdf),  
1124 1996.

1125 Federal Environment Agency: National Inventory Report for the German Greenhouse Gas  
1126 Inventory 1990–2019, available at: <https://unfccc.int/documents/194930>, (last access:  
1127 15 December 2022), 2021.

1128 Fernandez, J. M., Maazallahi, H., France, J. L., Menoud, M., Corbu, M., Ardelean, M., Calcan,  
1129 A., Townsend-Small, A., van der Veen, C., Fisher, R. E., Lowry, D., Nisbet, E.G.,  
1130 Röckmann, T.: Street-level methane emissions of Bucharest, Romania and the  
1131 dominance of urban wastewater., *Atmospheric Environment: X*, 13, 2590-1621,  
1132 100153, <https://doi.org/10.1016/j.aeaoa.2022.100153>, 2022.

1133 Fredenslund, A.M., Scheutz, C., Kjeldsen, P.: Tracer method to measure landfill gas emissions  
1134 from leachate collection systems, *Waste Management*, 30, 2146-2152,  
1135 <https://doi.org/10.1016/j.wasman.2010.03.013>, 2010

1136 Fredenslund, A. M., Rees-White, T. C., Beaven, R. P., Delre, A., Finlayson, A., Helmore, J.,  
1137 Allen, G., Scheutz, C.: Validation and error assessment of the mobile tracer gas  
1138 dispersion method for measurement of fugitive emissions from area sources, *Waste  
1139 Management*, 83, 68-78, <https://doi.org/10.1016/j.wasman.2018.10.036>, 2019.

1140 Federal Environment Agency: National Inventory Report for the German Greenhouse Gas  
1141 Inventory 1990 – 2018, available at: <https://unfccc.int/documents/226313> (last access:  
1142 30 March 2022), 2020.

1143 Hendrick, M. F., Ackle, R., Sanaie-Movahed, B., Tang, X., Phillips, N. G., Fugitive methane  
1144 emissions from leak-prone natural gas distribution infrastructure in urban  
1145 environments, *Environmental Pollution*, <https://doi.org/10.1016/j.envpol.2016.01.094>,  
1146 2016.

1147 Hou, Q., Yang, D., Li, X., Xiao, G. and Ho, S. C. M., Modified Leakage Rate Calculation  
1148 Models of Natural Gas Pipelines, *Mathematical Problems in Engineering*,  
1149 <https://doi.org/10.1155/2020/6673107>, 2020.

1150 Jackson, R. B., Saunio, M., Bousquet, P., Canadell, J. G., Poulter, B., Stavert, A. R.,  
1151 Bergamaschi, P., Niwa, Y., Segers, A. and Tsuruta, A., Increasing anthropogenic  
1152 methane emissions arise equally from agricultural and fossil fuel sources,  
1153 *Environmental Research Letters*, 15, 071002, [https://doi.org/10.1088/1748-  
1154 9326/ab9ed2](https://doi.org/10.1088/1748-9326/ab9ed2), 2020.

1155 Jackson, R. B., Down, A., Phillips, N. G., Ackley, R. C., Cook, C. W., Plata, D. L., and Zhao,  
1156 K., Natural Gas Pipeline Leaks Across Washington, DC, *Environ. Sci. Technol.*, 48, 3,  
1157 2051–2058, <https://doi.org/10.1021/es404474x>, 2014.

1158 Kirchgessner, D. A., Lott R. A., Cowgill, R.M., Harrison, M. R., Shires, T. M., Estimate of  
1159 methane emissions from the U.S. natural gas industry, *Chemosphere*,  
1160 [https://doi.org/10.1016/S0045-6535\(97\)00236-1](https://doi.org/10.1016/S0045-6535(97)00236-1), 1997.

1161 Keyes, T., Ridge G., Klein, M., Phillips, N., Ackley, R., Yang Y., An enhanced procedure for  
1162 urban mobile methane leak detection. *Heliyon*. 9; 6 (10):e04876.  
1163 <https://doi.org/10.1016/j.heliyon.2020.e04876>, 2020.

1164 Lamb, B. K., McManus, J. B., Shorter, J. H., Kolb, C. E., Mosher, B., Harriss, R. C., Allwine,  
1165 E., Blaha, D., Howard, T., Guenther, A., Lott, R. A., Siverson, R., Westburg, H., and  
1166 Zimmerman, P., Development of atmospheric tracer methods to measure methane  
1167 emissions from natural gas facilities and urban areas, *Environmental Science &  
1168 Technology* 29 (6), 1468-1479 <https://doi.org/10.1021/es00006a007>, 1995.

1169 Lamb, B. K., Edburg, S. L., Ferrara, T. W., Howard, T., Harrison, M. R., Kolb, C. E.,  
1170 Townsend-Small, A., Dyck, W., Possolo, A., and Whetstone, J. R., *Environmental*  
1171 *Science & Technology* 49 (8), 5161-5169 <https://doi.org/10.1021/es505116p>, 2015.

1172 Luetschwager, E., von Fischer, J. C., Weller, Z. D., Characterizing detection probabilities of  
1173 advanced mobile leak surveys: Implications for sampling effort and leak size estimation  
1174 in natural gas distribution systems. *Elementa: Science of the Anthropocene*; 9 (1):  
1175 00143. <https://doi.org/10.1525/elementa.2020.00143>, 2021.

1176 Liu, C., Liao, Y., Liang, J., Cui, Z., Li, Y., Quantifying methane release and dispersion  
1177 estimations for buried natural gas pipeline leakages, *Process Safety and Environmental*  
1178 *Protection*, <https://doi.org/10.1016/j.psep.2020.11.031>, 2021.

1179 Maazallahi, H., Fernandez, J. M., Menoud, M., Zavala-Araiza, D., Weller, Z. D., Schwietzke,  
1180 S., von Fischer, J. C., Denier van der Gon, H., and Röckmann, T.: Methane mapping,  
1181 emission quantification, and attribution in two European cities: Utrecht (NL) and  
1182 Hamburg (DE), *Atmos. Chem. Phys.*, 20, 14717–14740, [https://doi.org/10.5194/acp-](https://doi.org/10.5194/acp-20-14717-2020)  
1183 [20-14717-2020](https://doi.org/10.5194/acp-20-14717-2020), 2020.

1184 Mahgerefteh, H., Oke, A., Atti, O., Modelling outflow following rupture in pipeline networks,  
1185 *Chemical Engineering Science*, <https://doi.org/10.1016/j.ces.2005.10.013>, 2006.

1186 MEEM, Methane emission estimation method for the gas distribution grid, [Online], Available  
1187 from: [https://www.dbi-](https://www.dbi-gut.de/emissions.html?file=files/PDFs/Emissionen/Final%20Report_MEEM%20DSO_end_signed.pdf&cid=5804)  
1188 [gut.de/emissions.html?file=files/PDFs/Emissionen/Final%20Report\\_MEEM%20DSO](https://www.dbi-gut.de/emissions.html?file=files/PDFs/Emissionen/Final%20Report_MEEM%20DSO_end_signed.pdf&cid=5804)  
1189 [\\_end\\_signed.pdf&cid=5804](https://www.dbi-gut.de/emissions.html?file=files/PDFs/Emissionen/Final%20Report_MEEM%20DSO_end_signed.pdf&cid=5804). (Last Accessed: 12 December 2022), 2018.

1190 Moloudi, R., Abolfazli Esfahani, J., Modeling of gas release following pipeline rupture:  
1191 Proposing non-dimensional correlation, *Journal of Loss Prevention in the Process*  
1192 *Industries*, <https://doi.org/10.1016/j.jlp.2014.09.003>, 2014.

1193 Mønster, J. G., Samuelsson, J., Kjeldsen, P., Rella, C. W., Scheutz, C., Quantifying methane  
1194 emission from fugitive sources by combining tracer release and downwind  
1195 measurements – A sensitivity analysis based on multiple field surveys, *Waste*  
1196 *Management*, 34, 1416-1428, <https://doi.org/10.1016/j.wasman.2014.03.025>, 2014.

1197 Myhre, G., Shindell, D., Bréon, F. M., Collins, W., Fuglestvedt, J., Huang, J., Koch, D.,  
1198 Lamarque, J. F., Lee, D., Mendoza, B., Nakajima, T., Robock, A., Stephens, G.,  
1199 Takemura, T., and Zhan, H.: Anthropogenic and Natural Radiative Forcing, in:  
1200 *Climate Change 2013: The Physical Science Basis, Contribution of Working Group I*  
1201 *to the Fifth Assessment Report of the Intergovernmental Panel on Climate Change*,  
1202 Cambridge, UK and New York, NY, USA, available at:  
1203 [https://www.ipcc.ch/site/assets/uploads/2018/02/WG1AR5\\_Chapter08\\_FINAL.pdf](https://www.ipcc.ch/site/assets/uploads/2018/02/WG1AR5_Chapter08_FINAL.pdf),  
1204 2013.

1205 Nisbet, E. G., Manning, M. R., Dlugokencky, E. J., Fisher, R. E., Lowry, D., Michel, S. E.,  
1206 Myhre, C. L., Platt, S. M., Allen, G., Bousquet, P., Brownlow, R., Cain, M., France, J.  
1207 L., Hermansen, O., Hossaini, R., Jones, A. E., Levin, I., Manning, A. C., Myhre, G.,  
1208 Pyle, J. A., Vaughn, B. H., Warwick, N. J., White, J. W. C., Very strong atmospheric  
1209 methane growth in the 4 Years 2014–2017: implications for the Paris agreement, *Global*  
1210 *Biogeochemical Cycles*, 33, 318 – 342, <https://doi.org/10.1029/2018GB006009>, 2019.

1211 Okamoto, H., Gomi, Y., Empirical research on diffusion behavior of leaked gas in the ground,  
1212 *Journal of Loss Prevention in the Process Industries*,  
1213 <https://doi.org/10.1016/j.jlp.2011.01.007>, 2011.

1214 Phillips, N. G., Ackley, R., Crosson, E. R., Down, A., Hutyra, L. R., Brondfield, M., Karr, J.  
1215 D., Zhao, K., Jackson, R. B., Mapping urban pipeline leaks: Methane leaks across  
1216 Boston, *Environmental Pollution*, 173, 1–4,  
1217 <https://doi.org/10.1016/j.envpol.2012.11.003>, 2013.



1218 Scheutz, C., Samuelsson, J., Fredenslund, A.M., Kjeldsen, P., Quantification of multiple  
1219 methane emission sources at landfills using a double tracer technique, *Waste*  
1220 *Management*, 31, 1009-1017, <https://doi.org/10.1016/j.wasman.2011.01.015>, 2011.

1221 Ulrich, B. A., Mitton, M., Lachenmeyer, E., Hecobian, A., Zimmerle, D., and Smits, K. M.,  
1222 Natural Gas Emissions from Underground Pipelines and Implications for Leak  
1223 Detection, *Environmental Science & Technology Letters*, 6 (7), 401-406,  
1224 <https://doi.org/10.1021/acs.estlett.9b00291>, 2019.

1225 Von Fischer, J. C., Cooley, D., Chamberlain, S., Gaylord, A., Griebenow, C. J., Hamburg, S.  
1226 P., Salo, J., Schumacher, R., Theobald, D., and Ham, J.: Rapid, Vehicle-Based  
1227 Identification of Location and Magnitude of Urban Natural Gas Pipeline Leaks,  
1228 *Environ. Sci. Technol.*, 51, 4091–4099, <https://doi.org/10.1021/acs.est.6b06095>, 2017.

1229 Weller, Z. D., Roscioli, J. R., Daube, W. C., Lamb, B. K., Ferrara, T. W., Brewer, P. E., and  
1230 von Fischer, J. C.: Vehicle-Based Methane Surveys for Finding Natural Gas Leaks and  
1231 Estimating Their Size: Validation and Uncertainty, *Environ. Sci. Technol.*, 52, 11922–  
1232 11930, <https://doi.org/10.1021/acs.est.8b03135>, 2018.

1233 Weller, Z. D., Yang, D. K., and von Fischer, J. C.: An open source algorithm to detect natural  
1234 gas leaks from mobile methane survey data, edited by: Mauder, M., *PLoS One*, 14,  
1235 e0212287, <https://doi.org/10.1371/journal.pone.0212287>, 2019.

1236 Weller, Z. D., Hamburg, S. P., and von Fischer, J. C., A National Estimate of Methane Leakage  
1237 from Pipeline Mains in Natural Gas Local Distribution Systems, *Environmental*  
1238 *Science & Technology*, 54 (14), 8958-8967, <https://doi.org/10.1021/acs.est.0c00437>,  
1239 2020

1240 Wiesner, S., Gröngröft, A., Ament, F. et al. Spatial and temporal variability of urban soil water  
1241 dynamics observed by a soil monitoring network. *J Soils Sediments* 16, 2523–2537.  
1242 <https://doi.org/10.1007/s11368-016-1385-6>, 2016

1243 Worden, J. R., Anthony Bloom, A., Pandey, S., Jiang, Z., Worden, H. M., Walker, T. W.,  
1244 Houweling, S., Röckmann, T., , Reduced biomass burning emissions reconcile  
1245 conflicting estimates of the post-2006 atmospheric methane budget, *Nature*  
1246 *Communications* 8, 2227 <https://doi.org/10.1038/s41467-017-02246-0>, 2017

1247 Yan, Y., Dong, X., Li, J., Experimental study of methane diffusion in soil for an underground  
1248 gas pipe leak, *Journal of Natural Gas Science and Engineering*,  
1249 <https://doi.org/10.1016/j.jngse.2015.08.039>, 2015.

1250 Yuhua, D., Huilin, G., Jing'en, Z., Yaorong, F., Evaluation of gas release rate through holes in  
1251 pipelines, *Journal of Loss Prevention in the Process Industries*,  
1252 [https://doi.org/10.1016/S0950-4230\(02\)00041-4](https://doi.org/10.1016/S0950-4230(02)00041-4), 2002.

1253